



## Review Article

# The diversity, frequency and severity of natural hazard impacts on subsea telecommunications networks

Lucy Bricheno<sup>a,\*</sup>, Isobel Yeo<sup>b</sup>, Michael Clare<sup>b</sup>, James Hunt<sup>b</sup>, Allan Griffiths<sup>c</sup>, Lionel Carter<sup>d</sup>, Peter J. Talling<sup>e</sup>, Megan Baker<sup>e</sup>, Stuart Wilson<sup>f</sup>, Matthew West<sup>f</sup>, Semisi Panuve<sup>g</sup>, Samuela Fonua<sup>g</sup>

<sup>a</sup> National Oceanography Centre, Joseph Proudman building, 6 Brownlow Street, Liverpool L3 5DA, UK

<sup>b</sup> National Oceanography Centre, European Way, Southampton SO14 3ZH, UK

<sup>c</sup> National Grid, UK

<sup>d</sup> Victoria University of Wellington, Aotearoa, New Zealand

<sup>e</sup> Departments of Earth Science and Geography, Durham University, UK

<sup>f</sup> Ocean-IQ, UK

<sup>g</sup> Tonga Cable Limited, Tonga



## ARTICLE INFO

## Keywords:

Natural hazards  
Subsea cables  
Compound hazards  
Telecommunications  
Climate Change

## ABSTRACT

Subsea cables underpin global communications, carrying more than 99 % of all digital data traffic worldwide. While this >1.6 million km-long network has been designed to be highly resilient, subsea cables can be damaged by a number of natural hazards that occur across all water depths in the ocean. Here, we explore the diversity of natural hazards that can damage cables, considering a broad frequency-magnitude spectrum. This paper is the first global perspective of actual and potential hazards affecting cables. As such, it is an accessible overview of the regional variability and complexity of hazards. Relatively rare and extreme events, such as super typhoons, submarine landslides or associated turbidity currents and volcanic eruptions, can synchronously cause widespread damage to multiple systems, in some cases disconnecting entire countries or dramatically slowing data traffic. We show that damage is rarely linked to an initial event, instead arising from cascades of processes that can lag by years. Not all instances of cable damage that relate to natural processes are linked to extreme events. We show that much smaller intensity meteorological and oceanographic processes such as storms and continuous seafloor currents that have been overlooked by previous studies can also damage subsea cables. New analysis of past instances of cable damage reveals that a significant proportion of previously unattributed faults may relate to such low-level but sustained impacts. It is these hazards that are most likely to change in frequency and magnitude in response to ongoing climate change but are also more predictable. Through mapping of exposure to these different hazards, we identify geographically-constrained hazard hotspots and identify various mitigation measures to enhance the evidence base and further strengthen subsea telecommunications network resilience.

## 1. Introduction

The global network is comprised of more than 1.6 million km of subsea telecommunications cables that underpin the internet, email, telephone communications, and trillions of dollars per day in financial transactions (Carter, 2009; Burnett and Carter, 2017). The term “network” is informally used here to cover over 400 different subsea cable systems carry more than 99 % of digital traffic and telecommunications worldwide (Burnett and Carter, 2017). This enabled the

effective transition to remote working during the COVID-19 pandemic (Talling et al., 2022a, 2022b). Improved global connectivity via the cable network can help progress towards several sustainable development goals (SDGs) defined in Morton et al. (2017): Reduce Inequality (SDG 10) & Decent Work and Economic Growth (SDG 8): remote working can help reduce inequality by allowing inclusive access to medicine and education, and promote economic growth by providing flexibility and opportunities to those limited by geography or access needs. Sustainable Cities and Communities (SDG 11) & Responsible

\* Corresponding author.

E-mail address: [luic@noc.ac.uk](mailto:luic@noc.ac.uk) (L. Bricheno).

<https://doi.org/10.1016/j.earscrev.2024.104972>

Received 10 May 2024; Received in revised form 23 October 2024; Accepted 31 October 2024

Available online 4 November 2024

0012-8252/© 2024 The Authors. Published by Elsevier B.V. This is an open access article under the CC BY license (<http://creativecommons.org/licenses/by/4.0/>).

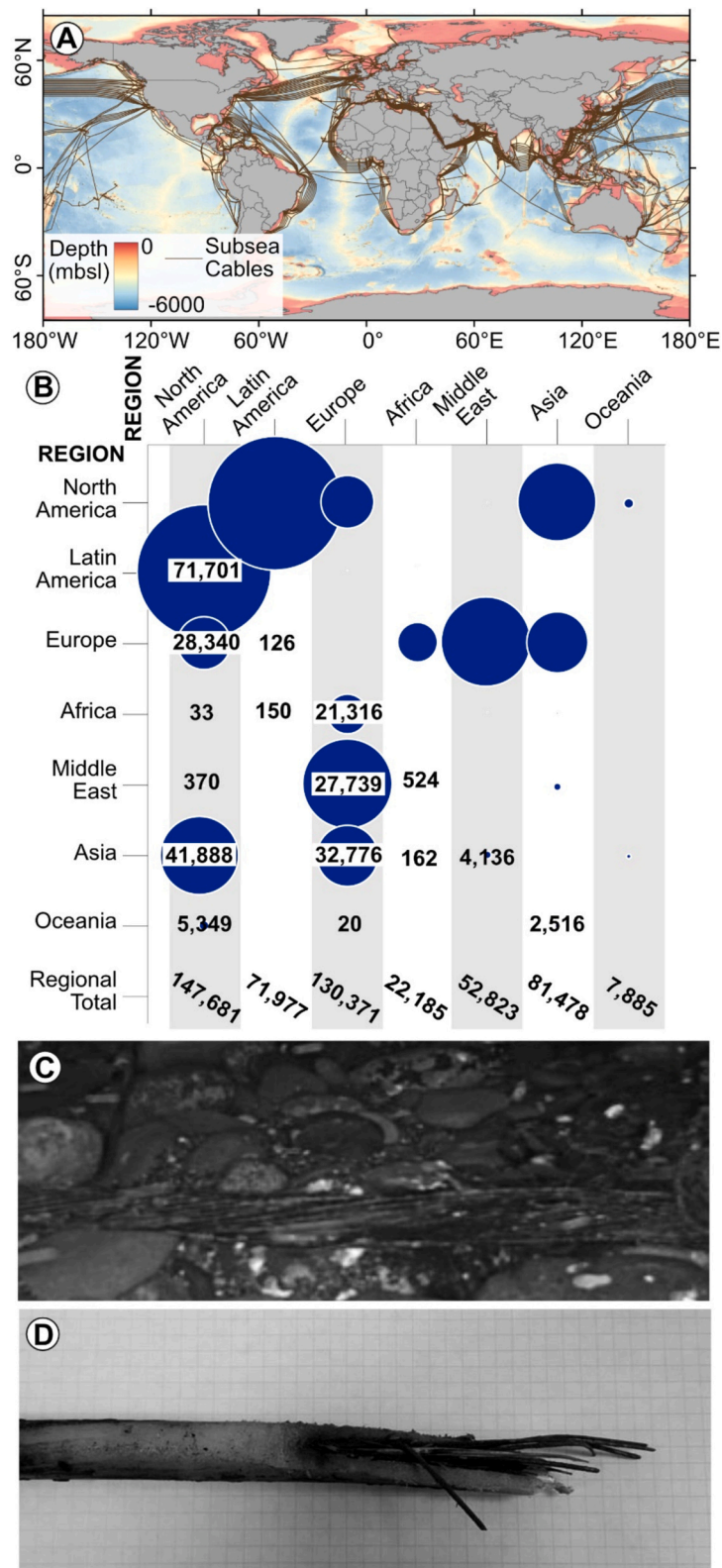


**Fig. 1.** Locations of subsea telecommunications cables and the data traffic capacity carried between different regions. [A] The locations of subsea telecommunications cables around the world (Telegeography, 2023). [B] The relative connection bandwidth available between different regions and the regional total bandwidth (Gigabytes per second). Some regions have no connectivity bandwidth to most areas of the globe, while others are robustly connected. Oceania is particularly vulnerable with both few connections and low total bandwidth. [C & D] Examples of seafloor cable damage. [E] Cumulative frequency plot of cable faults relative to water depth and attributed to different causes. This plot shows how different causes of cable faults show a different frequency distribution relative to water depth, with fishing and anchoring-related faults occurring dominantly in very shallow waters, largely limited to the continental shelf and upper continental slope. While abrasion and chafe-related faults are most prone in shallower waters, such damage can occur in deeper waters. Natural hazards, including earthquakes, landslides and other natural processes, appear to operate independent of water depth.

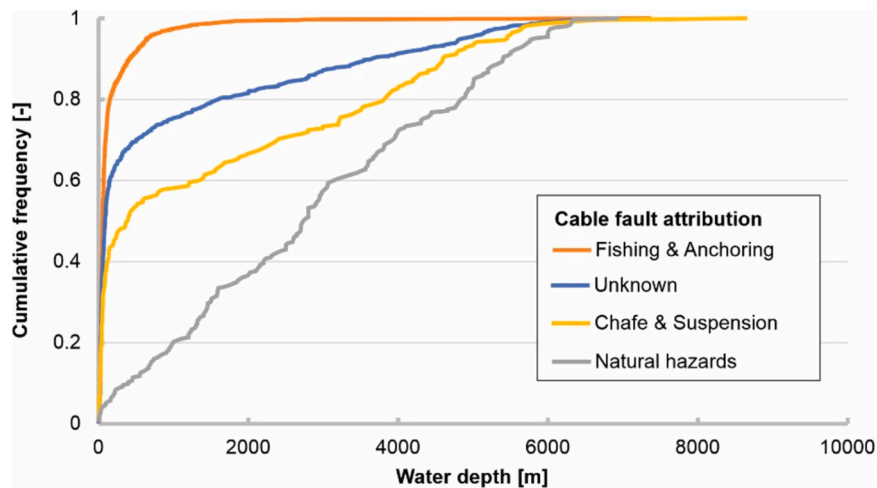


Fig. 1. (continued).

Consumption and Production (SDG 12): work-from-home culture and online meetings can alleviate urban congestion and the need for (long distance) travel. Overall reduced carbon emissions through these routes with contribute to progress on Climate Action (SDG 13), while better global connectivity supports Partnerships for the Goals (SDG 17) through improved regional and international cooperation, capacity building and access to science, technology and innovation.

On a global scale, the subsea cable network (Fig. 1A) is remarkably resilient. Redundancy from multiple systems, and a diversity of landings can reduce vulnerability and secure redundancy during potential breaks (GDIP, 2024). To further reduce risk, routes are carefully planned to minimise exposure to natural hazards, and because cables may be armoured or buried in shallow waters or where hazards are known but cannot be easily avoided (Carter et al., 2014). Thus, key to resilience is understanding the nature of these hazards and locations where they are likely to occur. This is particularly challenging for natural hazards that can cause widespread damage, but for which there are few observed examples due to their relative infrequency or sparsity of observable coverage. This has implications for new cable routes in frontier areas where prior experience does not exist e.g. Wilson (2013). However, as the cumulative length of subsea cables continues to increase worldwide, accompanied by a growing need to better connect remote and vulnerable communities, the exposure to natural hazards will increase. While the global network is resilient, the resilience of the network varies between and within regions, owing to geographical / geological variations in hazard intensity, exposure and the diversity in routes and landing stations available (Fig. 1B). While Europe and North America have abundant inter-connections, some countries in less populated regions such as Oceania are reliant on relatively few, or even a single-point cable connection, making them more vulnerable to the impact of natural hazards.

Analyses of global databases reveal that the most commonly recorded damage (hereafter referred to as ‘cable faults’) relate to accidental human activities (Fig. 1E). These incidents are primarily caused by anchor drops and interaction with bottom fishing equipment, and occur in shallow water (< 200 m); e.g. Kordahi and Shapiro, 2004, Kordahi et al., 2007, 2016). Fig. 1E shows increased likelihood of abrasion and chafe-related faults in shallower waters, while earthquakes, landslides and other natural processes, appear to operate independent of water depth. While only 25 % of all faults are directly attributed to environmental (hereafter natural) hazards (Carter, 2009; Clare et al., 2023), such events can be particularly significant as they can synchronously damage long lengths of multiple cable systems across large areas (Lasley et al. (2007), Gigacom (2012), in some cases isolating entire regions (Carter et al., 2014, Cattaneo et al., 2012 Gavey et al., 2017; Ericson et al., 1952;

Hsu et al., 2008). While infrequent, the impacts of natural hazards on subsea cables have been acutely demonstrated several times in recent decades. Following the explosive submarine eruption of Hunga Volcano in 2022, the only international cable that connected the Kingdom of Tonga to the rest of the world was damaged, cutting off international connectivity and hampering aid efforts at the critical moment for response (Clare et al., 2023; Seabrook et al., 2023). In 2020, a large flood of the Congo River triggered a powerful seafloor sediment-laden flow (a ‘turbidity current’) that ran out for >1100 km into the deep sea at speeds of 5–8 m/s, damaging multiple seafloor cables and crippling internet connections from west to south Africa during the earliest stages of the COVID-19 pandemic lockdown (Talling et al., 2022a, 2022b). In 2006, a total of 21 cable faults occurred offshore Taiwan as a result of underwater landslides triggered by the Pingtung earthquake, and an associated longer runout turbidity current travelling at 5–16 m/s. These cable breaks took 11 cable ships (almost half of the world’s entire fleet) seven weeks to complete the repairs, costing hundreds of millions of US dollars (Carter et al., 2014). Natural hazards that cause high-profile, damaging, extreme events have generally been the focus of research and case studies. However, there is growing evidence that lower magnitude, but more sustained, long-term impacts can also be damaging (Kordahi et al., 2019; Clare et al., 2023). To date, no study has taken a holistic approach to consider the full gamut of natural hazards, which range from extreme one-off events to progressive impact from sustained low-intensity stressors.

Natural hazards occur over the entire range of ocean depths, from the coast to the deepest hadal trenches, and include both geological (e.g. volcanic or seismic in origin) and hydrological (e.g. weather or oceanographic in origin) hazards. While there is range of different natural hazards and a range of frequencies and magnitudes to consider for each, these are also likely not consistent through time and subject to change. Natural hazard impacts can be complex, compounded, and cascading in nature, and few studies have examined these more complicated scenarios. Our new work will set-out the characteristics of these “3 Cs”: complex, compounded, and cascading, and their implications to the hazard exposure of the cable network. Complex, where several physical processes are involved: Compound, as multiple stressors are acting together; and Cascading, due to chain reactions in the natural environment. For example, the 2018 eruption of Anak Krakatau volcano (Indonesia) that resulted in the collapse of part of its submarine flank and triggering of a damaging and fatal tsunami, coincided with an unrelated, major storm, which inhibited effective emergency response and recovery from the tsunami (Ye et al., 2020). In the case of the 20,223 eruption of Hunga Volcano (Kingdom of Tonga), the explosive eruption generated a tsunami that inundated coastal communities in Tonga, as

well as triggering the seafloor density currents that severed critical subsea telecommunications cables at a critical time (Clare et al., 2023). A better understanding is needed of the frequency, intensity, and location of hazards, as well as how multiple factors may combine and interact resulting in more serious later outcomes for subsea telecommunication cables. In this study we look at the whole range of natural hazards over a spectrum of characteristics (frequency, exposure duration, and impact). These hazard characteristics can be transient due to changing controlling factors. Of these, anthropogenically-influenced climate change is the compounding factor which is subject to the greatest magnitude of change and associated uncertainty. For example, the frequency and severity of meteorologically driven natural hazards has changed, and will continue to change, as a result of anthropogenically-influenced climate change (e.g. Gallina et al., 2016). A recent global review summarised the diverse range of meteorologically-driven natural hazards influenced by climate change whose impacts may threaten subsea cables (Clare et al., 2022); including, but not limited to: 1) increased frequency and severity of storms, which can damage cables directly through wave action onshore and where the wave base approaches the seafloor in shallow water (<200 m); 2) increased frequency and height of storm surges, which can damage cable landing stations and/or cause flooding and mobilise seabed sediments; 3) increased likelihood of and severity of river flooding, which in turn transports sediment from coast to ocean; 4) coastal erosion which can damage landing stations and cause submarine mass movement events (landslides); 5) ice-related hazards, such as seafloor scouring by iceberg keels, in high latitude regions.

In this work we analyse an industry database of 5817 cable faults recorded between 1965 and 2019. We identify those cable faults attributed to natural processes, and make use of publicly available datasets to constrain the conditions or combination of factors that resulted in the cable fault. To illustrate the diversity of hazard scenarios, we first present several specific case studies, and then demarcate regions that are most likely to experience hazardous events or conditions. In many entries throughout the database, a specific trigger could not be readily attributed to a cable fault, and such cases were marked “Unknown”. We aim to make use of additional data to provide new insights into some of their origins. This study aims to identify and attribute past cable faults caused by natural hazards, through forensic examination of instances of past cable damage, and contextualise these incidents within a database of natural hazards to better determine the geographical/geological variations in exposure of the subsea cable network to such threats, and hence the broader implications for resilience. This work differs from and complements previous studies of cable faults that were either local case studies (e.g. Talling et al., 2022a, 2022b; Clare et al., 2023), focused on individual hazard types (e.g. earthquakes or tropical storms; Pope et al., 2017a, 2017b), or future effects of meteorological, climate-driven hazards (Clare et al., 2023). This present study synthesises prior and new case studies, complementing and extending those other global studies, and providing information of relevance to industries that strive to design resilient seafloor infrastructure and stakeholders responsible for critical national infrastructure. The instances of cable damage presented herein provide unique insights into diverse seafloor processes, and their connections to atmospheric, terrestrial and other processes, that could otherwise go unknown due to the paucity of monitoring in the deep ocean.

## 2. Cable faults database, analysis and complementary datasets

To understand how different natural hazards can damage subsea telecommunications cables, we analyse a unique 40-year industry database provided by Global Marine Limited that documents past instances of cable faults on the global network. This database attributes cable faults to broad categories. In order to focus on natural hazards, we eliminate those cable breaks that were attributed directly to human activities including fishing, dredging, anchor drops, technical faults, and

seabed mining. This leaves 1473 faults (25 %) in the database that could be attributable to natural hazards. The seven categories included in the industry database are: “Cable”; “Landslides”; “Chafe”; “Other Nature”; “Seismic”; “Suspension”; “Unknown”. These categories were assigned by the repair company recovering the cable and therefore typically dependent on physical evidence, for example fishing equipment caught around the cable, or clear evidence for a natural event, for example local detectable seismicity. This evidence is harder to find for some categories and is necessarily inferred on the basis of the best information available. For example, evidence of a subsea landslide in an area that is not monitored may be inferred either by the pattern of cable damage (e.g. sequential faults progressively into deep water), from bathymetry data if it is available (not usually the case) or from other possible causes like seismicity (e.g. Heezen and Johnson, 1969; Piper et al., 1999; Hsu et al., 2008; Carter et al., 2014). As a result, some of the faults attributed to certain natural processes may be miscategorised. Some further information on the seabed conditions is provided for many faults, which can aid with recategorization if required. It is important to note that the database only includes data for cable faults that caused a halt in data transmission and/or major repair, but may not include information on more minor repairs or maintenance in instances where that occurred. The database includes information on the time and date of the fault, the location, water depth, cable type, seabed type (where known), and other relevant metadata.

The slightly arbitrary nature of classification classes means there is potentially some overlap between different classifications. For example, a cable fault attributed to a seismic event may actually be caused by a landslide or turbidity current that was triggered by the seismic event. There is also a lot of diversity hidden within the “Other Nature” category, particularly associated with faults relating to wave and current activity (for example cable faults labelled “Storm Damage”, “struck by heavy object from tropical storms”, and “Cyclonic activity”). Section 3 focussed on case study events that were clearly attributable to three different categories of natural hazards. These case studies were then used to define parameters that indicate a risk to subsea cables and these were mapped globally.

Our analysis of cable faults also included cross-reference to a number of other global datasets, including:

- i) Bathymetry: Global bathymetric data were downloaded from the General Bathymetric Chart of the Oceans (GEBCO) at 1/12th degree resolution. Localised higher resolution datasets were downloaded for comparison as required from the Generic Multi-resolution Topography Map Tool (GMRT.com) and from GeoMapApp. Bathymetry products (slope and terrain ruggedness index (TRI) defined by Riley et al. (1999)) were generated from both higher and lower resolution grids but the lower grid resolution values were used for global comparison because they are available across all the oceans, making global vulnerability comparisons possible. While the values for slope and TRI were lower for the lower resolution datasets, representing a smoothing of features by the gridding algorithm, in almost all cases where they were compared, regions with higher slopes and TRI in the higher resolution bathymetric datasets correlated with higher but less pronounced values in the 1/12th degree resolution data. Different wavelengths of roughness are relevant for subsea cables, large wavelengths of tens to hundreds of metres increase the likelihood of cable suspension, increasing its vulnerability to other phenomena and abrasion of the cable where it re-joins the seafloor, while smaller wavelengths, of millimetres to meters increase the chances of abrasion on the cable in rocky regions. While only the larger wavelengths are captured in the GEBCO data, they are often associated with finer scale roughness as a result of the exposure of rocky seafloor through faulting or in regions of rough volcanic terrain.



- ii) Storm track information: This data comes from International Best Track Archive for Climate Stewardship (IBTrACS). Developed collaboratively with all the World Meteorological Organization, IBTrACS is the most complete global collection of tropical cyclones available. It merges recent and historical tropical cyclone data from multiple agencies to create a unified, publicly available, best-track dataset that improves inter-agency comparisons (Knapp et al., 2010).
- iii) Wave frequency and magnitude: The wave data used in this report is taken from models run at the UK National Oceanography Centre. The WaveWatch III™ spectral wave model, version 3.14 (Tolman, 2009) was used to simulate historic wave conditions. The global model has an approximate horizontal resolution of 80 km by 40 km; Atmospheric forcing (surface winds) was taken from the ERA Interim reanalysis. The model was run continuously from January 1979 – December 2015. Hourly significant wave height (Hs) is used for our analysis. The full configuration and methodology is available from Bricheno and Wolf (2018). Using the observed latitude and longitude of the cable fault, we search for corresponding closest point in the global models of surface wave conditions. The Hs on the day of the cable break event is considered, and the maximum value taken. To put these values in context, the multi-decadal data are used to calculate a 90th percentile wave height to represent the extreme events.
- iv) Ocean Currents: Currents are taken from the GLORYS12V1 product is the CMEMS global ocean eddy-resolving (1/12° horizontal resolution, 50 vertical levels) reanalysis covering the altimetry (1993 onward). It is based largely on the current real-time global forecasting CMEMS system. The model component is the NEMO platform driven at surface by ERA data. More information and data download can be found at doi: [10.48670/moi-00021](https://doi.org/10.48670/moi-00021). Daily mean currents are extracted for the lowest active model grid box of the 50 standard levels.
- v) Seismicity: Earthquake magnitude data were extracted from the United States Geological Survey earthquake catalogue (<https://earthquake.usgs.gov/earthquakes>) for all recorded events with a magnitude >5 to between 2013 and 2023, which provides a globally representative view of the geographic variation in seismic intensity. Data were projected and displayed in QGIS (QGIS Development Team, 2020) for comparison with cable and cable fault locations.
- vi) Volcanic Eruptions: Only a few breaks in the database are attributable to volcanic activity, and for these we referred specifically to published literature for that eruption. The global distribution of known volcanoes (both active and inactive) was downloaded from the Smithsonian Global Volcanism Program (Venzke, 2013 <https://volcano.si.edu/>). Data were projected and displayed in QGIS (QGIS Development Team, 2020).
- vii) River sediment flux: data for total river discharge and sediment flux to the coastal ocean were taken from Milliman and Farnsworth (2013). Data were projected and displayed in QGIS (QGIS Development Team, 2020).
- viii) Canyons: were defined as steep-walled, sinuous valleys with V-shaped cross sections. Data extracted from the morphology database (Harris and Whiteway (2011)) which characterises geomorphic features and the zones within the ocean where they occur.
- ix) Cable location: The locations of cables were defined using the proprietary database provided by Global Marine Limited. This database has also been used to assess hazards in specific areas (Pope et al., 2017a, 2017b) and to investigate climate change-related impacts on subsea telecommunications (Clare et al., 2022). As the database is proprietary it is not shared here. Illustrative locations are shown from the open-access Telegeography dataset (Telegeography, 2023 <https://www.submarinecablemap.com/ready-for-service/2023>).

### 3. Results

#### 3.1. Global view and classification

The faults identified from the cable fault database fall into two main categories, those caused by a sudden catastrophic event, and those caused by longer term interaction with hostile conditions in the natural environment. The catastrophic events are responsible for 13 % of the faults that could be attributable to natural hazards. This is broken down into 2 % landslides, 11 % seismic. While faults are likely caused by continuous exposure to a harsh marine environment make up 14 % (chafe = 11 % and suspension 3 %). Faults classified as ‘cable (7 %)’ may have experienced damage through either route, and are not further defined. The remaining categories are ‘other nature = 3%’, leaving the final 62 % categorised as “unknown”. These processes are dealt with separately in the following sections, however, they may interact in reality to increase regional vulnerability.

##### 3.1.1. Short period catastrophic hazards

Earthquakes, volcanic eruptions, interaction with ice, and submarine landslides or turbidity currents are all examples of actual and potentially catastrophic hazards that can impact subsea cables. There are 211 cable faults attributed to ice, landslides and seismic causes (which include three volcanic activity related faults), alongside a further volcanic activity fault in an “Other Nature” category. It is important to emphasise that the fault classifications are designated in the database at the time of recovery and maintenance. With little time for analysis there is potential confusion and misclassification at this stage. We recommend that more detailed information together with photographs are collected in future, to further classify faults and improve attribution (particularly in terms of natural hazards). These cable faults represent 15 % of all the natural/unknown incidents, or 43 % of the faults with a definite natural cause (excluding the unknown category).

Earthquakes can physically displace the seafloor hundreds of kilometres away from the epicentre, as a fault or slope instability which may in turn generate tsunamis capable of transiting ocean basins (Pope et al., 2017a, 2017b). Submarine landslides can be triggered from slope instabilities caused by earthquakes, but also by many other processes; for example, in areas of rapid sediment accumulation (Pope et al., 2017a, 2017b; Bailey et al., 2021). Rapid sediment accumulation can occur on the steep flanks of fjords, offshore from river mouths, in submarine canyons, on the flanks of volcanic ocean islands, and other sites (e.g. Hampton et al., 1996). These mix with the ambient seawater to create fast-moving turbidity currents (which may also form from plunging sediment-laden river flood water; Carter et al., 2014). In high latitudes, iceberg calving and its interaction with the seabed may also directly damage subsea cables or even generate localised slope failures that have wider reaching impacts (e.g. Normandeau et al., 2021). While rarer than the other hazards mentioned, volcanic eruptions both above and below water can generate a variety of hazards, including extreme temperatures, explosions, lava flows, physical displacement of the seafloor and pyroclastic density currents. Eruptive processes can generate associated cascading hazardous processes, such as triggering landslides, generating lahars or causing tsunamis (e.g. Tanguy, 1994).

There is no specific category in the database for storm related faults although they are mentioned in both “suspension” and “other nature” categories. As for geological hazards, storm activity can both directly and indirectly damage seafloor cables through deepening and intensifying wave activity on the seafloor, by increasing river discharge, by introducing terrigenous material into the marine environment from flooding, and/or damage to fishing equipment that may entangle cables making them more prone to failure (e.g. Carter et al., 2012). There are also two separate “repeater” faults attributed to lightning in the database, and there may be others that are unrecorded.

The complexity of the interactions and connections between these causal factors, and other natural processes, means that establishing the

primary cause of a cable fault can be challenging. This is exacerbated by potential lag times between these connected events. For example, studies offshore from rivers have shown there can be lag times of hours to many months between maximum river discharge and the initiation of slope failures or turbidity currents. This delay is because slope instability was preconditioned by high sediment discharge from the river loading slopes, but the landslide's final trigger may be a smaller environmental perturbation such as extreme water level changes at spring tides or low level seismicity (e.g. Clare et al., 2016; Gavey et al., 2017; Pope et al., 2017a, 2017b; Talling et al., 2022a, 2022b).

### 3.1.2. Longer period environmental impacts on cables

Suspension and chafe-related faults are primarily caused by hydrodynamic loads acting on the cable in adverse seafloor conditions. The ideal approach is to avoid laying cables in suspension at all, but sometimes this is unavoidable, for example during installation in areas of variable bathymetry, especially in deep water where slack control is difficult. Suspension and chafe cable faults account for 14 % of all the potentially natural hazard-related faults identified in our database, and almost half (46 %) of those faults when the unknown category is removed. Suspension means part of a cable is not in contact with the seafloor. This can occur where (i) cables are moved, (ii) underlying sediments are eroded or (iii) the seabed has rough, rocky topography. Once suspended, the cable then can abrade rapidly at the contact points at each end of the suspension as the unsupported section moves in the currents. Additionally, the suspended cable is much more vulnerable to other hazards such as fishing activity. Chafe faults result from physical abrasion of the cable, which physically weakens it and allows the ingress of seawater eventually causing an electrical fault short and/or breakage of the glass fibres.

Suspension and chafe can be caused by the action of currents on the cable and/or surrounding seafloor. Benthic currents can generate sediment movement such as sand waves, and significantly erode the seafloor, exhuming previously-buried cables, while high sediment loads combined with high current speeds can potentially drag and abrade unbundled cables at seafloor. Sustained wave action in shallow water areas, especially those with rocky substrates, can increase abrasion. Such rough and irregular terrains create a more hostile environment in which long term movement of the cable over these rocks can enhance wear and tear. Tidal currents are a particular threat in these environments, because their combination of strength, regularity over a month but variability on an hourly-timescale tends to move a cable back and forth over the same area, creating a "sawing" effect.

Such rough topography is also the areas where suspensions are more common and a cable may be supported by topographic highs. If benthic currents are sufficiently strong and frequent, the suspension will move with the flow causing the cable to fatigue at its suspension points. Thus, when considering natural hazards to cables, ocean currents, waves and seabed type should also be taken into account.

However, not all suspension or chafe faults are necessarily caused by long-term processes. For example, a submarine landslide may also lead to cable suspension, or short-term extreme wave action during a storm could cause enough abrasion on a cable to cause a fault (e.g. Carter, 2009; Carter et al., 2014; Talling et al., 2022a, 2022b). Repeated storm action over a period of time may also progressively increase the likelihood of a fault. Thus, both chafe and suspension faults may also be the result of catastrophic events, and again the complexity of these interactions can make it difficult to attribute to a single cause. Ice can also pose a long-term cascading hazard, such as frazil ice accumulating on surface laid cable and lifting it into suspension in the water column or moving it over adjacent rocks, making it more vulnerable to abrasion or other risks (Clare et al., 2022).

### 3.2. Illustrative examples of cable damage from major natural hazards

We now present three recent examples of cable faults that are

directly attributable to major natural events, to illustrate the diverse and cascading hazards that can damage subsea cables. i) The 2022 eruption of Hunga Volcano – a short-period catastrophic hazard offshore from the Kingdom of Tonga; ii) the cascading multi-hazards experienced in the Congo Canyon, offshore West Africa in 2020; and iii) major storm-driven marine events during tropical storms. These cases are selected as representing distinct geological (Hunga volcano), hydrological (Congo Canyon), meteorological, and oceanographic (tropical storms) aspects. The ordering of the case studies moves from high-impact, low likelihood events, down to more common, but less consequential natural hazards.

#### 3.2.1. Extensive subsea cable damage resulting from the Hunga Volcano eruption in 2022

Hunga Volcano (previously known for the Hunga Tonga-Hunga Ha'apai caldera rim vents) is an almost entirely submerged caldera volcano around 60 km northwest of Tongatapu in the Kingdom of Tonga (Fig. 2). The volcano has been regularly active over the past few decades, with eruptions in 1998, 2009, 2014–2015 and, most recently, in 2021–2022. While most of its eruptions have been relatively low on the volcanic explosivity index (VEI; a measure on log scale between 0 and 8 of the explosivity and volume of a volcanic eruption), the 2021–2022 activity culminated in an eruption exceeding VEI 5 (representing an ejecta volume of >1 km<sup>3</sup>), which generated tsunami waves with run ups over 15 m (Lynett et al. (2022), Pakoksung et al. (2022)), released an eruption plume over 57 km high, that reached into the mesosphere (Proud et al. (2022)) and catastrophically damaged the two subsea telecommunications cables that serve the islands of Tonga (Clare et al., 2023).

The 2021–2022 eruption sequence began on the 20th December, with the first weeks primarily characterised by low explosivity, small Surtseyan eruptions, which produced steam-rich gas and ash plumes with heights of up to 20 km. However, on the 15th January 2022, at 17:13 (local time) a  $M_w$  4.1 earthquake was detected near the volcano, followed by major explosions ( $M_w$  5.6 to 5.8) at 17:15 and 17:20. A well-developed umbrella cloud was present by 17:17 and column collapse (material thrown upwards into the eruption plume that lost buoyancy and fell vertically into the ocean) began at around 17:20. Data transmission stopped on the domestic seafloor telecommunications cable at 17:30, and on the international cable at 18:44 (Fig. 2D). Subsequently during cable repair, it was found that 105 km of the domestic cable, and 89 km of the international cable, had either been damaged or buried beneath volcanic material to such a depth it could not be recovered.

Seafloor surveys in the months following the eruption demonstrated that column collapse had generated vast underwater flows, which reached distances of more than 100 km from the vent and travelled at speed up to 122 km/h, the fastest underwater currents that have ever been measured (Clare et al., 2023; Seabrook et al., 2023). These flows accelerated down gullies on the submerged flanks of the volcano, in places eroding depths of up to 100 m, and then deposited lobes of volcanoclastic sediment on slopes below 10 degrees. The cables were buried, in places, by more than 20 m of volcanic sediments, rendering them unrecoverable and complicating repair efforts, which required the manufacture of large lengths (>100 km) of cable; well beyond what would usually be required for a repair. The remoteness of the region added complications in the time for the repair vessel to get to site and for shipping of the new cable. Repairs on the international cable were completed, as a result of collaboration between multiple companies, within 5 weeks of the damage, while it took almost 18 months for the domestic cable to be repaired. This underlines the need for backup communications, such as low-level satellite communications; however, satellites carry <1 % of the bandwidth capacity of cables and, in the case of Hunga volcano, could not be used until five days after the eruption due to the obstruction created by the volcanic plume.

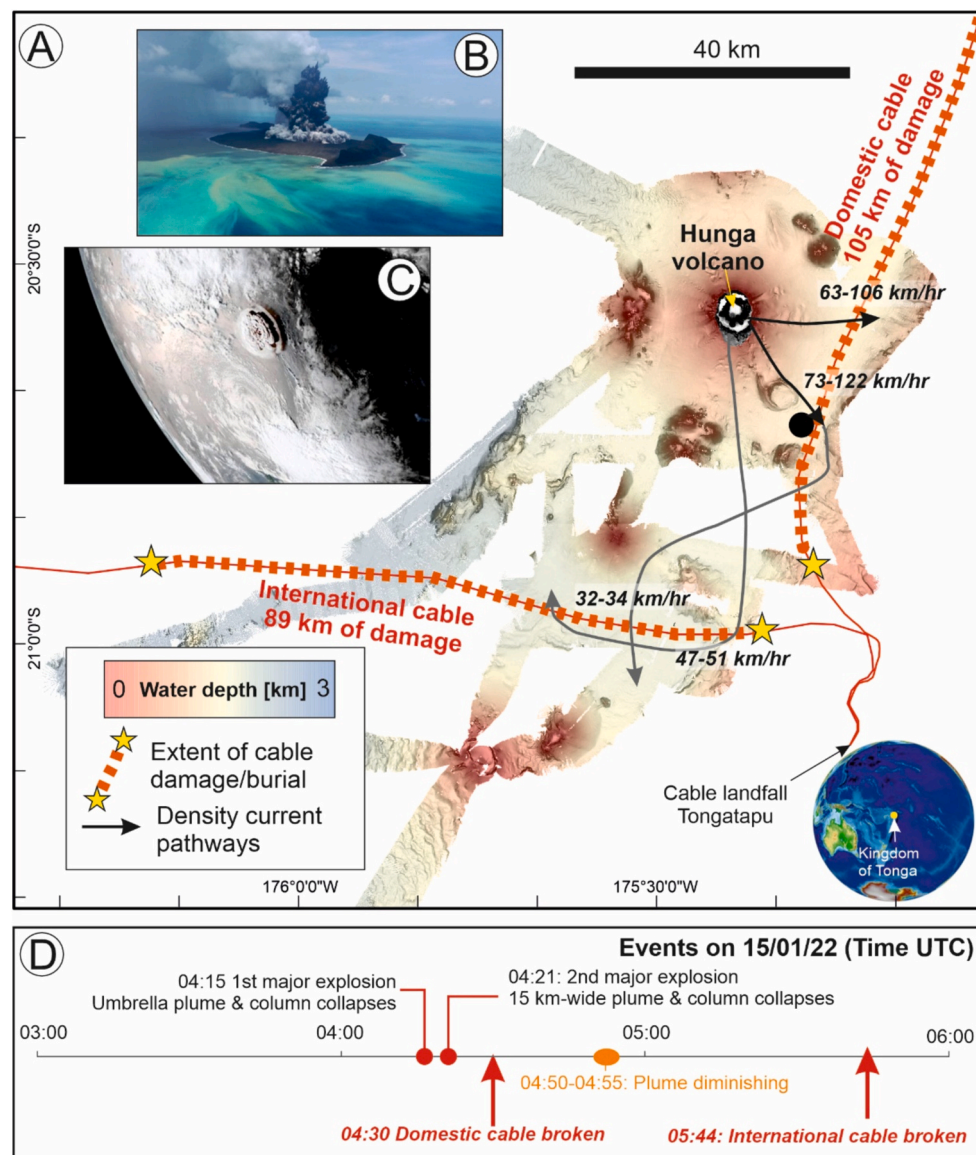


**Fig. 2.** Subsea cable damage caused by the January 2022 eruption of Hunga volcano, Kingdom of Tonga. [A] Seafloor relief in the area around Hunga Volcano after the 2022 eruption, showing the locations of the subsea cables (modified from Clare et al., 2023). The dashed lines show the lengths of cable that were buried beyond recovery during the eruption. [B] Image taken of the eruption before the major January 15th 2021 climax (Tonga Geological Services). [C] The January 15th event as viewed from space [NASA]. [D] A simplified timeline of the eruption and cable interruptions on January 15th 2021.

### 3.2.2. Repeated and multiple cable breaks resulting from major flood-primed turbidity currents in the Congo Submarine Canyon

The Canyon lies offshore West Africa, where its head extends about 30 km inside the estuary of the Congo River, directly connecting one of the world's major rivers with a submarine canyon that extends around 1200 km along its sinuous course into the deep sea. At ~2000 m water depth the canyon transitions to a less incised channel that continues downslope to the depositional lobe at ~5000 m water depth. (Talling et al., 2022a, 2022b; Fig. 3). Due to the vast length of the submarine Congo Canyon, several subsea cables have been routed across the canyon, rather than around it. Between 1883 and 1937, telegraphic cables were laid across the upper reaches of the canyon in water depths shallower than 2 km (Heezen et al., 1964). These cable routes experienced frequent faults, which recurred preferentially during periods when the discharge from the Congo River was elevated, interpreted to relate to powerful turbidity currents (Heezen et al., 1964). In more recent years, modern fibre optic cables were laid across the canyon in deeper water, including the SAT-3 system (South Atlantic 3, laid in

2001) at a water depth of around 3570 m, and two branches of the WACS cable (West Africa Cable System, laid in 2012), crossing at around 2000 m and 4000 m water depth. These cables, which had previously been undamaged for 18 years, were damaged by unusually powerful and long runout (>1100 km) turbidity currents in January and March 2020. The latter of these events occurred during the first COVID-19 lockdown when data and telecommunications traffic were particularly important (Talling et al., 2022a, 2022b). Here, cable repairs took around 15 to 20 days due to the need to mobilise a vessel and undertake complex repairs in such deep water. Unlike the Hunga Volcano-related cable damage, it was possible to reroute data traffic via a redundant link on another cable system, demonstrating the value of diverse cable route options. The damaging turbidity currents occurred after a large flood of the Congo River, which resulted in a peak discharge of more than 70,000 m<sup>3</sup>/s at the end of December 2019, representing the largest Congo flood for almost sixty years (Talling et al., 2022a, 2022b). However, the turbidity currents that caused the cable damage (and whose arrival was detected by deep-sea sensors) occurred 2 weeks and 10 weeks respectively after



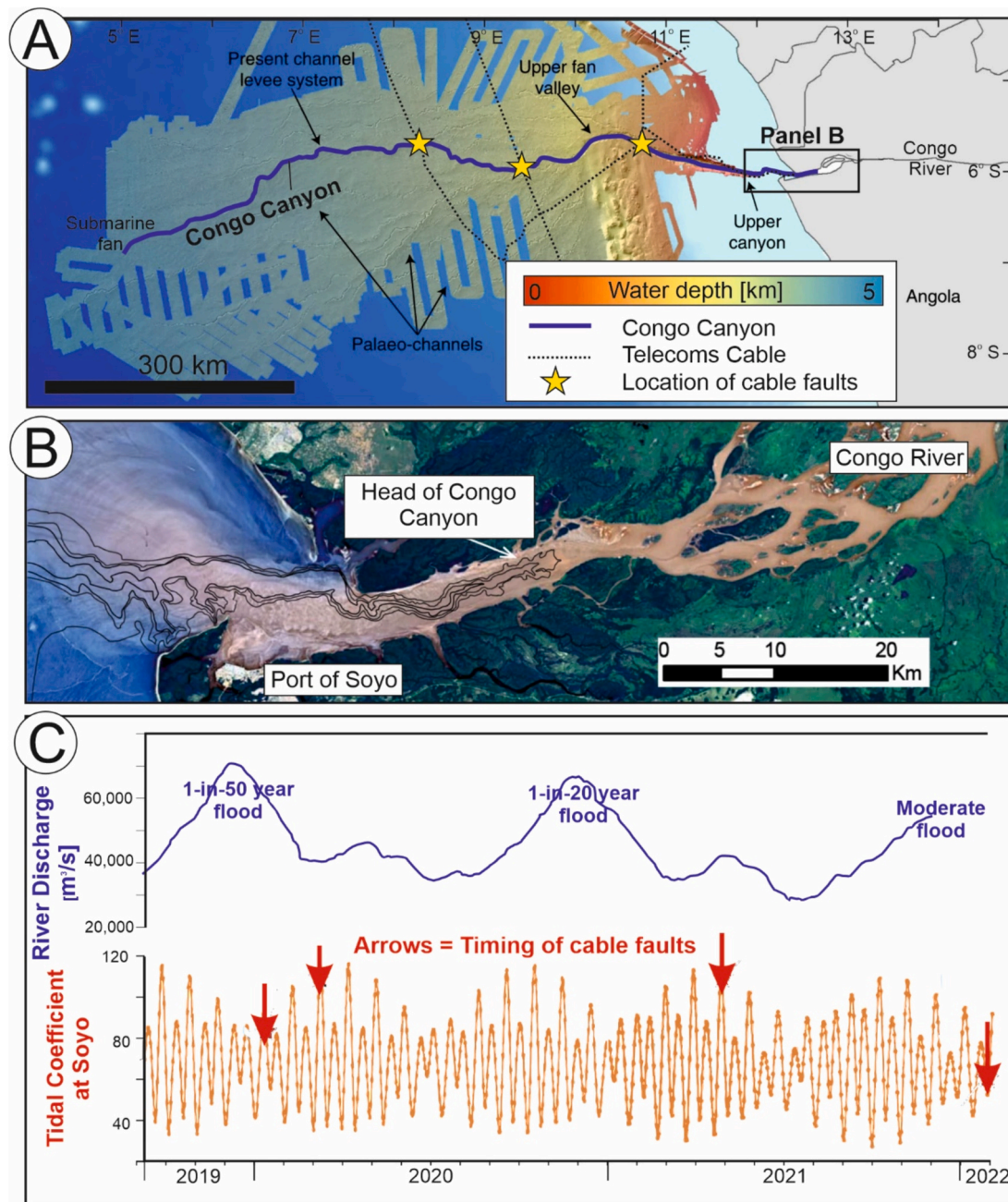


**Fig. 3.** Locations of cable damage at crossings of the submarine Congo Canyon following major flooding of the Congo River. [A] Extent of the Congo Submarine Canyon system that extends to a submarine fan in around 5 km water depth. Seafloor relief is shown, overlain with a simplified version of the canyon-channel system (blue line) with locations of subsea cables shown as dashed black lines and cable faults as stars (modified from Pope et al. (2022)). [B] More detailed view showing the head of the Congo Canyon that reaches up into the Congo River estuary (modified from Talling et al., 2022a, 2022b). [C] Time series showing the water discharge of the Congo River at the Kinshasa gauging station and tidal coefficient relative to major flooding events and the timings of subsea cable faults. (For interpretation of the references to colour in this figure legend, the reader is referred to the web version of this article.)

the peak in the flood discharge. It is thought that the large volumes of sediment that were delivered to the river mouth during the flood accumulated at the head of the canyon and were then remobilised, and flushed seaward during the major spring tides (Talling et al., 2022a, 2022b). A more recent, but similarly powerful turbidity current that broke one or more cables occurred in April 2021, January 2022 and August 2023. However, by August 2023 a new (Equiano) cable system had been routed into deeper water, away from the Congo Canyon, which survived, enabling rerouting of data traffic within just two hours, to minimise further disruption (WIOCC, 2023).

### 3.2.3. Cable damage due to meteorological and oceanographic hazards

Storm waves generated by winds at the ocean surface might seem far removed from impacts on seabed infrastructure. However, energetic waves, particularly those with long periods, can penetrate deeply, generating large shear stresses on the seabed sometimes in water depths of 100 s of m (Huthnance et al., 2002; Madsen et al., 1993). A single storm can pass over the course of a few hours (high-latitude storms) or last for days for lower-latitude storms including hurricanes and typhoons (Carr III and Elsberry, 1995). The impacts of storm waves can also be linked to the state of tide, as this can modulate water depth, exposing or protecting the seabed. Therefore, it is important to consider



the timing of a storm in the context of tidal water levels, and the combined stresses of wave and tidal currents on the seabed. Large storms passing over areas of shallow water can generate large wave and current stresses at the seabed. Proximity to shore /shelf gives access land derived material which can be mobilised by high wind/wave events.

Faults in subsea cables caused by oceanographic and meteorological hazards are often overlooked or misattributed as being geological in their origin. In order to identify historic cable breaks that may be attributable to marine hazards, we interrogated the global cable fault database in conjunction with modelled wave data. For every cable fault, a time series of significant wave height (Hs) and mean period was extracted from the wave data outlined in section 2. To find potential candidates for storm conditions, we select events where Hs exceeded the 99th percentile wave height previously experienced at this site (throughout a 37 year hindcast). A total of 98 faults appear to be strong candidates for cables being damaged during unusually high storm waves. Within the database we analysed, 17 % of those classified as 'cable' and 9 % of 'unknown' faults meet the criteria outlined above.. Likely candidates are not just those classified 'unknown' but have been labelled as cable, chafe, and suspension. This raises the awareness that other marine natural hazards may pose a greater threat to the cable network than those previously dominantly attributed to geological processes.

**3.2.3.1. Cable damage during tropical storms.** Several individual storm events were investigated, based on high wave-conditions experienced co-incident with observed cable faults. On 5th September 2006, a cable fault occurred off the coast of Japan in 45 m water depth after the category 5 super typhoon Ioke passed. At the fault site during this event, the modelled significant wave height reached 4.5 m, with long-period swell waves up to 16.8 s in period, which equates to a bottom orbital velocity of 0.825 m/s (which is fast enough to mobilise very coarse sand or pebbles). However, a detailed repair report revealed that, though the timing is suspicious, it seems that the fault was due to a high voltage blowout within a joint, not an external cause. Therefore, it is deemed unlikely that the fault was caused by the storm (unless by lightning strike which is not unprecedented).

On 3rd July 2001 a cable fault occurred on the Asia Pacific Cable Network 2 (APCN-2) off the coast of Taiwan in 1518 m water depth. At this site the cable is surface-laid on a muddy seafloor. The cable fault occurred during the passage of typhoon Utor, which at peak storm intensity was classed as a category 1-equivalent typhoon. We analysed the wave data for storm Utor in the same way as storm Ioke. At the peak of the storm, wave heights of 8 m occurred, coincident with long period swell waves with periods in excess of 12 s. However, the deep water at this site kept bottom orbital velocities experienced at the seafloor below 0.4 m/s throughout the storm. Though not a very strong storm, it brought heavy rain and associated landslides. It was thus possible that this fault was caused by cyclone-triggered sediment density flow. However, the industry installation report explained that the fault was thought to have been caused by external aggression as the cable had been twisted with damage to the armour wires, and appears result of an item catching the cable and causing tension rather than abrasion, and the precise cause is therefore equivocal.

On 15th February 2006, a broad low-pressure system moved from the east of Madagascar towards Réunion Island. The storm was relatively weak, classified as a Tropical Cyclone. The maximum windspeed reached was 50 knots and a low pressure of 991 mb was recorded on February 19th at 6 pm. Wave conditions coincident with the cable break were relatively calm (below 2 m significant wave height). However, this storm generated very heavy precipitation. Réunion Island experienced extreme, 1-in-50-year rainfall rates, with a station in the capital Saint-Denis recorded 376 mm within a 3-h window. On the 19th February a cable fault was experienced on SAFE seg 6 (South Africa Far East), less than 6 km off the coast of Réunion Island. The fault occurred on a section

of surface-laid, semi-armoured cable in a water depth of 1214 m, which was classified in the database as a Suspension fault. The seafloor was described as rugged, with steep topography and sandy substrate. This location had previously experience faults in both 2001 and 2002 In this latest instance, the cable was abraded allowing seawater to intrude causing a "shunt fault". The repair report for SAFE Seg 6 noted that the seabed was very mobile with many sand waves, and the cable was found suspended between two sand waves when recovered. An extended section (27 km) of cable was noted to be damaged, and entangled by debris and fresh green-coloured vegetation. In some sections there appears to have been a rockfall onto the cable as well. This was specifically noted to have been attributable to recent tropical storms and heavy rainfall.

These examples of genuine storm damage, and two "false positive" examples demonstrate how difficult attribution can be for meteorological and oceanographic damage to cables. Pope et al. (2017) aimed to identify cable break events related to tropical cyclone activity, finding 35 possible candidates between 1989 and 2015. Utor was included in this analysis, with the cable break coincident with the storm passing offshore Taiwan. The two false positives were previously classified as 'Unknown' in the cable fault database, and the event at Réunion was recorded as Suspension. It is only by combining the natural hazards exposure, and detailed repair reports that we can present a full picture of fault attribution.

### 3.3. Global overview and exposure of subsea cables to marine natural hazards

The cable industry is familiar with abrasion faults, but the mechanisms that caused them are not often further explored. Suspension and chafe cable faults account for 14 % of all the potentially natural hazard-related faults identified in our database. To connect these faults with ocean current speeds, it is useful to breakdown the faults observed by water depth. In water depths shallower than 200 m there are 82 faults (47 %), for intermediate depths (200 m-2 km) 36 faults (21 %) are recorded, and 55 faults (32 %) at locations deeper than 2 km. Similarly, we can assess those faults caused by suspension, in this case the distribution is more balanced. There have been 19 in depths shallower than 200 m, 13 in intermediate depths, and 20 in >2 km water. Wave exposure during regular storms can be well quantified, and large storms predicted in the near-term with good accuracy, allowing regions where cables may be impacted to be delineated. By combining these different parameters, we can begin to identify regions of the oceans that are likely to be less hospitable to subsea cables. These results highlight the abundance and extent of marine generated natural hazards from currents and waves.

#### 3.3.1. Combining seafloor currents and seabed morphology to assess exposure to abrasion

On average, the abyssal currents experienced by cables are typically very slow, of the order of a few millimetres per second Zenk (2008). However, shallow water areas (particularly in tide-dominated regions) can experience fast seabed flows in excess of 1 m/s. Tidal flows can also combine with large non-tidal residuals, formed for example by meandering ocean eddies. Low-level fatigue through exposure to ocean currents is the cause of relatively few cable faults, however the exposure is much more predictable. Very few studies have been conducted on subsea cable failures caused by sustained wear-and-tear. Yet, Dinmohammadi et al. (2019) find corrosion and abrasion to be responsible for over 40 % of failures in subsea power cables. Mapping this hazard is therefore a valuable step forward for avoiding abrasion risk, especially for new transoceanic routes for telecommunications in frontier areas.

In certain circumstances, seafloor currents can lead to cable suspension, strumming of the cable, and its movement across a rough or hard seabed on rough or hard seafloor, particularly where the currents direction is orthogonal or oblique to the cable axis that can lead to abrasion and fatigue, particularly when sustained for protracted periods

of time. In the case of armoured cables in shallow water depths (< 1000 m), it is initially the outer polypropylene yarns that are severed, which starts to unravel in the current. This unravelling then exposes the armour wires to the seabed current, which can wash away the protective galvanised coating. Seawater can then corrode the unprotected armour wires that hydrolyse and dissolve, exposing the lightweight cable at its core. This inner lightweight cable (which is also equivalent to the unarmoured cables deployed in >1000 m water depth) is sheathed in polyethylene insulation, which can be further abraded, such that seawater infiltrates the metallic core, causing a short circuit (known as a shunt fault). While it is possible for extremely vigorous and sediment-laden currents (such as those in the Congo canyon and offshore Tonga) to cause such damage almost instantaneously, this mode of failure can also develop over prolonged periods of time due to the sustained or repeated action of seabed currents (Dinmohammadi et al., 2019). Fig. 4 demonstrates typical cable damage from chafe experienced in areas of high current. In panel [B] the outer wire layer has been abraded away and the inner wires show the distinctive flattening like they've been

severely abraded. Note that in this case, this wasn't the fault location, and is for illustration purposes only.

Chafe and abrasion are caused by a combination of forcing from flow moving across rough seabed. Therefore, to understand this exposure, we must combine maps of seabed roughness and current speed. The resolution of modelled deep-ocean current is relatively low, but it is possible to map currents on a broad scale across regions that are likely to experience the most energetic currents at seafloor. Since the launch of Seabed2030 <https://seabed2030.org/>

(Mayer et al., 2018), almost 25 % of the world oceans' seafloor has been sampled for depth. The best resolution data available come from either Smith and Sandwell (1997) who base their 1–12 km dataset on satellite altimetry and ship depth soundings, or the GEBCO\_2023 Grid with a resolution of 15 arc-seconds (100 s m). Using global maps, larger regions of rough topography can also be mapped and compared to cable routes and currents to identify potential hotspots of rough seabed exposed to high current speed. To identify areas where cables are more exposed to abrasion, we combine information on seabed roughness with the square of the seabed current speed to provide a value for seabed stress, following the classic drag equation formulated by Rayleigh (1880). Source data for the currents are described in Section 2. We map

regions where there is co-location of strong current stresses and irregular seabed relief that may be most prone to abrasion (Fig. 5). This mapping highlights areas of exposure that include: those i) around mid-ocean ridges; ii) affected by deep western boundary currents; iii) potential abrasion hot-spots in the Caribbean, arising from the complex seafloor relief created by volcanic island arcs; iv) where the trans-Atlantic cables cross the Gulf Stream; v) where trans-Pacific cables cross the Kuroshio Current; vi) stretches of the Red Sea / Persian Gulf where many cables are exposed to deep ocean currents (Telegeography, 2023).

We can then interrogate this exposure map to contextualise the faults recorded in the database. To do this, the seabed stress is extracted at each location corresponding to an incident of chafe or suspension. This population is then compared with the 'background' distribution of the whole ocean dataset. Table 1 shows the background distribution of abrasion risk across the whole global ocean (background population) compared to the site-specific stress experienced at location of chafe and suspension faults. Consistently higher abrasion exposure is observed in the chafe and suspension populations compared to the background population, supporting the interpretation that energetic currents and rough topography are significant risk factors at these faults.

High-speed current events which far exceed the background known as "benthic storms" (Aller, 1989) may be a potential cause for some groups of abrasion faults observed at deep oceanic sites. Benthic storms are created primarily by deep cyclones beneath Gulf Stream meanders (Hollister and McCave (1984), Gardner et al. (2017)) generating sufficient bed-shear stress to erode and resuspend sediment. The area where this seems very likely to have occurred is in the western North Atlantic, south of Greenland (Woodgate and Fahrback, 1999) but there are likely to be others.

As well as the current speed and direction, the amount and nature of the bedload are also important stressors. Bedload and suspended sediment transport may induce cable abrasion, suspension, burial and exhumation. In sandy regions, stirring may result in cable burial, while scour may expose cables to potentially hazardous boulder/rock substrates. (e.g. Carter et al., 1991). Maps presented in Fig. 5 will likely still underestimate the risk from abrasion: Low resolution bathymetry maps might miss small-scale surface roughness like boulders where the macro-surface is flat but sediment hasn't been allowed to accumulate due active hydrodynamics. In this case, the currents are the creator of the abrasive surface, so naturally there might be areas of bare rock / coarse

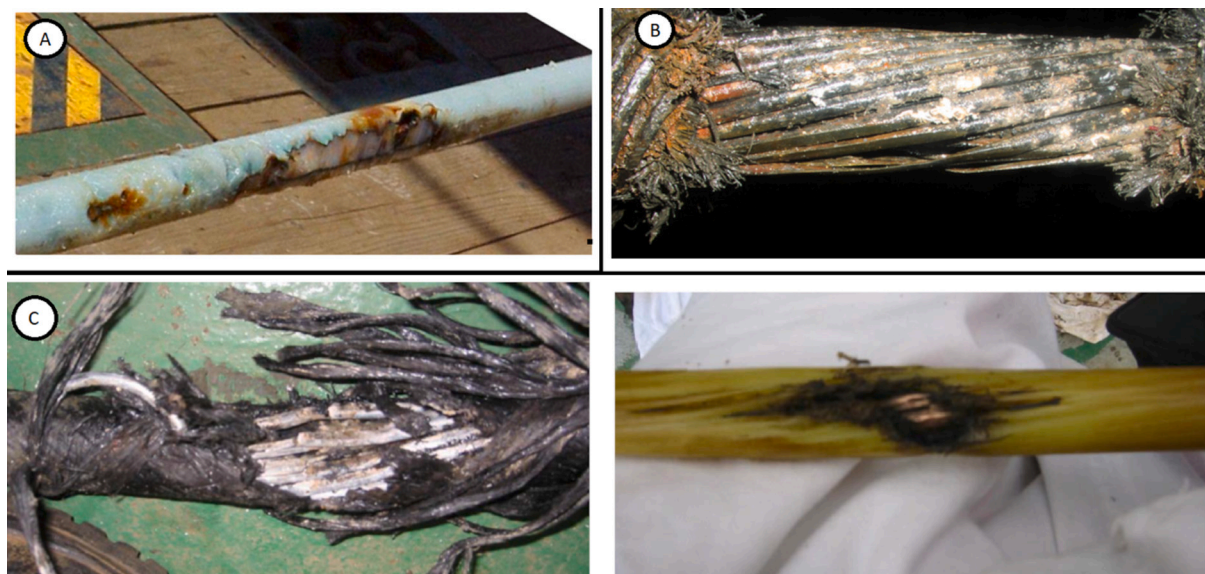
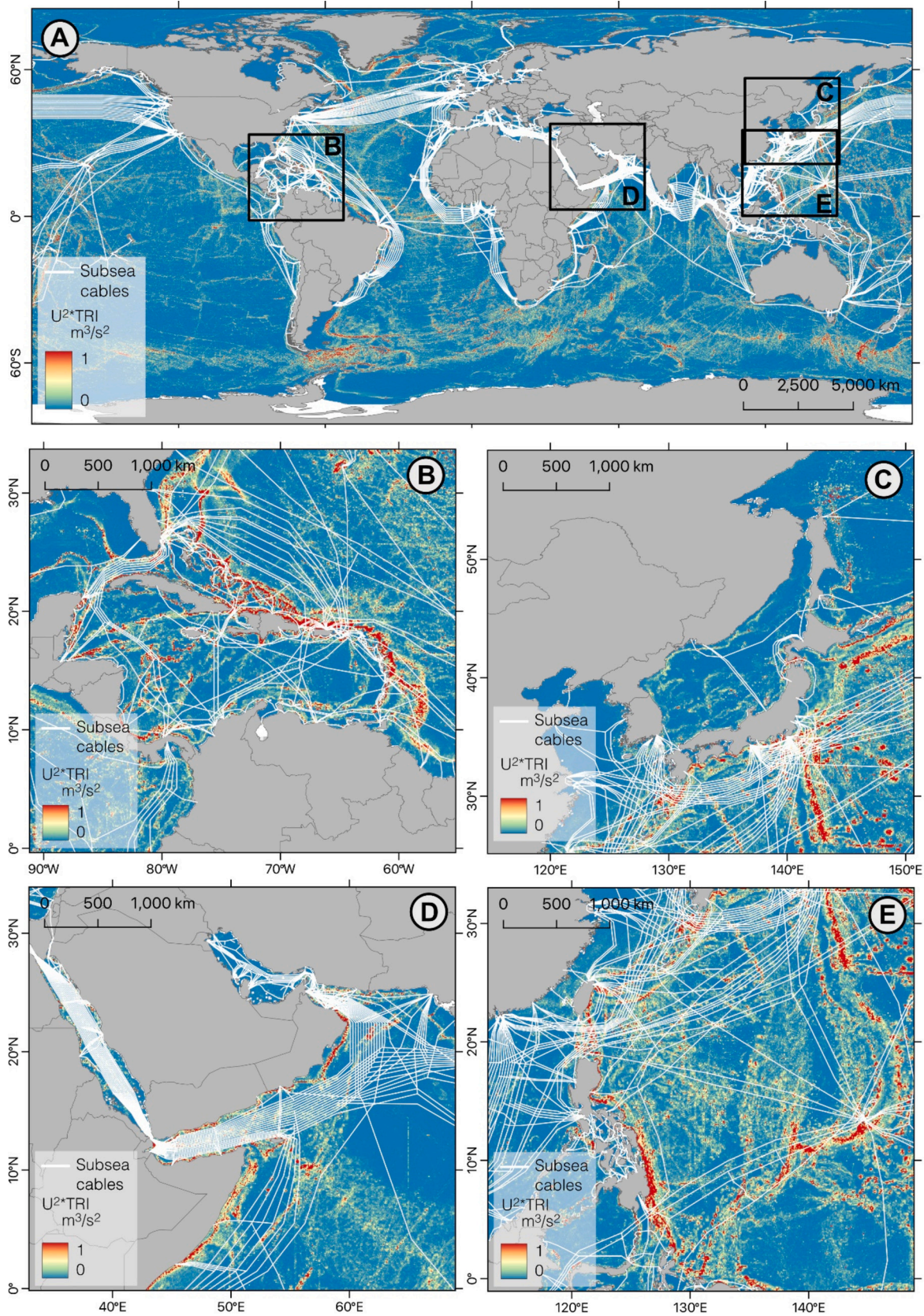


Fig. 4. Typical damage from chafe experienced by different cable types experience in areas of high current. [A] prolonged abrasion of lightweight cable in deep water leading to shunt fault. [B] Abrasion damaged experienced by a (now rarely used) rock armour cable. [C] focussed abrasion of semi-armoured cable (left), leading to a chafe fault exposing the core and shunt fault (right).





**Fig. 5.** [A] Combined global abrasion risk map of combined deep ocean current speed squared and seabed rugosity [ $m^3 s^{-2}$ ] with the approximate cable locations (Telegeography, 2023); [B-E] The same data shown at smaller scale in for regions with particularly high likelihood of conditions conducive to abrasion in the Gulf Stream and Caribbean Seas, Kuroshio Current, Caribbean Seas, and the Philippines.



**Table 1**

Frequency of occurrence of abrasion risk factor coincident with chafe and suspension faults, compared with background population.

Abrasion risk ( $\text{m}^3\text{s}^{-2}$ )	<0.25	0.25	0.5	0.75	1.0	1.5	2.0	2.5	3.0	3.5	$\geq 4.0$
Background population (%)	84.8	10.4	2.2	0.9	0.6	0.4	0.2	0.1	0.07	0.05	0.1
Chafe (%)	58.6	15.9	5.5	6.2	2.1	4.8	2.1	2.8	0.79	0	1.4
Suspension (%)	63.6	18.2	4.6	0	4.6	4.6	2.3	2.3	0	0	0

substrate associated with sites of fast-moving currents. For abrasion to occur requires a combination of a hard substrate and strong currents. Thus, very high-resolution mapping of the seabed is needed, for an accurate risk assessment. Even where the abyssal seabed is composed of more common oozes and muds, if two cables cross one another where variable near-seabed currents exist, there is also a risk of mutual abrasion between the two.

### 3.3.2. Identifying regions exposed to greatest wave energy at seafloor

As seen section 3.2.3, subsea cables may also be vulnerable to the impact of storm generated sea waves. Waves with long period and large significant wave height are more energetic. Energy generated by sea surface waves reaching the seabed has been observed as deep as 200 m (Huthnance et al., 2002). By generating seabed stresses, these waves can mobilise sediment that also has a linear component e.g. wind drift, tides. As a result, the combined flow, exposes or buries cables, leading to localised suspension, or generating abrasive seafloor currents (Allan, 2000). To map this risk factor, we calculate wave energy ( $H_s^2/T/m$ ) divided by water depth (Fig. 6). The wave data used here are annual mean significant wave heights and energy period over a 37 year hind-cast. This gives an indication of how much wave energy reaches the seabed globally. Shelf seas are most exposed to the greatest wave energy, particularly the ‘ocean’ facing side rather than the enclosed seas. These

regions are where long-fetch waves that have grown over large areas of ocean meet the coast. Long swells that cross ocean basins can become decoupled from the location of the storm tracks themselves. This non-local nature of waves means that a global approach is needed to classify the risk.

The dataset of wave exposure was interrogated in the same way as current exposure in section 3.31, however, no clear relationship was found between wave exposure and chafe or suspension faults. Combined with section 3.2.3a, our analysis has not found any evidence to suggest that sea-surface waves are a threat to subsea cables. In contrast to continuous ocean currents, waves exert forces only during short period events, which are not well represented in the mean climate. Nonetheless, short-lived, periodic benthic storms are known to impact the seabed. E.g. Gardner et al. (2017) find seabed disturbances generated by meso-scale eddies, and fast-moving hurricanes or tropical storms. Therefore, there is still some value in mapping areas where energy generated by surface processes are more likely to reach the seabed.

The broad Northwest European shelf (Fig. 6B) features large areas exposed to high relative wave energy. This region is by far the most exposed, with shallow waters experiencing frequent strong mid-latitude storms, whilst there is also a high density of cables. Seas around Southeast Asia (Fig. 6C) have an interesting combination of geography, with two different sets of risk factors. First, the steep narrow shelves

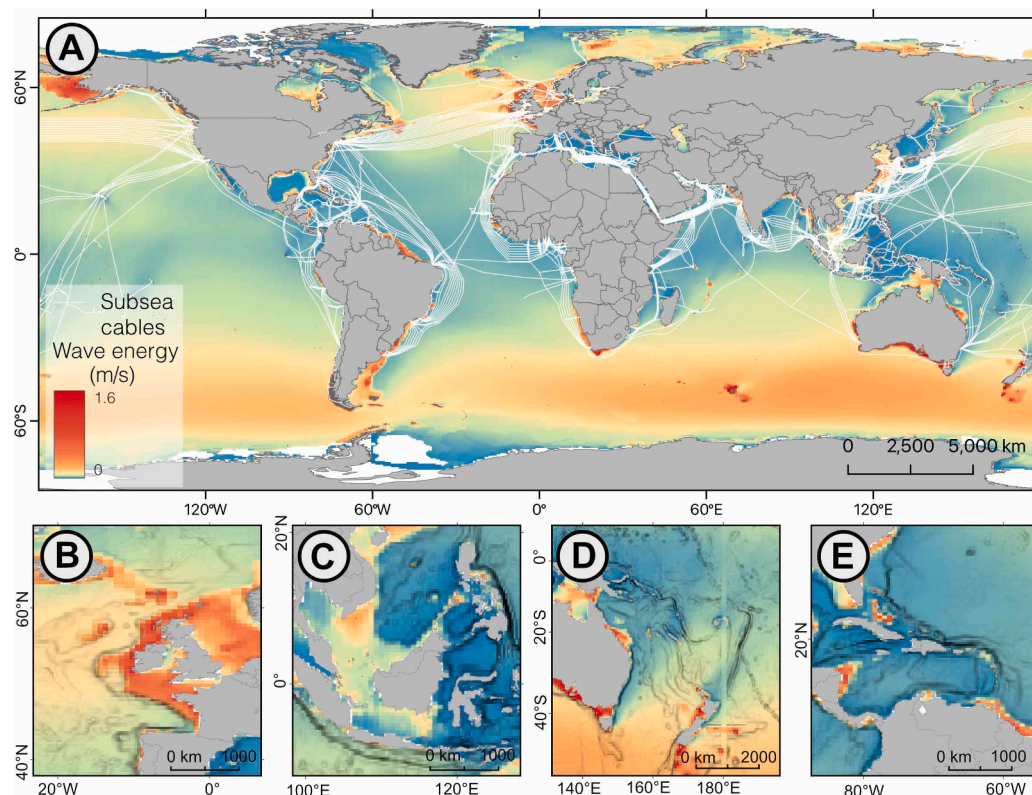


**Fig. 6.** Global risk map of wave energy at the seabed with the approximate cable locations [A]. Cable locations as presented by Telegeography, are overlaid in white. Wave energy is defined as a combination of wave energy and ocean depth defined as  $H_s^2/T/Z$ ; where  $Z$  is water depth,  $H_s$  is significant wave height, and  $T$  is wave period energy. [B-E] The same data shown at smaller scale in for regions with particularly high likelihood of conditions conducive to abrasion from both wave and tides: the Northwest European Shelf, SE Asia, Eastern Australia and New Zealand, and the Caribbean Seas. Note that wave energy data in panels B-E is overlain on a hillshaded seafloor relief to highlight the influence of seafloor relief.



around the Philippines where some hotspots of high wave energy reach the coast. Second, a wider, more exposed area of shallow water in the South China Sea which hosts many subsea cables. The Southern Ocean (Fig. 6D) has persistently large wave energy; with stretches of uninterrupted ocean, waves can grow around the globe, setting-up a high wave exposure even in deep waters (Snodgrass et al., 1966). Although there is little subsea infrastructure of any type present in the Southern Ocean, these large waves could affect stretches of offshore South Australia, and connections between Australia and New Zealand, and may affect new proposed systems to connect to Antarctica (e.g. Howe et al., 2022). In the Caribbean Seas, and offshore East Coast USA (Fig. 6E), wave impacts are constrained to the narrow shelf, where steep bathymetric relief allows deep water waves close to the coast. So, although hurricanes track across this entire region, the wave impacts experienced at the seabed are limited, as most of the seabed lies below the depth that is exposed to vigorous wave energy.

## 4. Discussion

### 4.1. Cascading hazards across a frequency-magnitude spectrum, and challenges in cable fault attribution

The analysis of past instances of cable faults reveals that a wide range of natural processes can pose a threat to subsea cables, spanning a broad frequency-magnitude spectrum. These include some of the most extreme events on Earth, such as the explosive eruption of Hunga volcano that resulted in extensive damage to subsea cables (Clare et al., 2023), and the powerful turbidity currents in the Congo Canyon that travelled >1100 km (Talling et al., 2022a, 2022b). In the case of such extreme events, the attribution of a cable fault is typically straightforward. However, the precise mechanism(s) that caused the damage to the cable may not necessarily be the initial event itself, but instead relate to subsequent chains of events that cascade from that initial event. For example, in the case of Hunga volcano, it was not the explosive eruption itself that caused the cable damage. Instead, the damage was caused by fast-moving seafloor density currents that were triggered when large volumes of dense pyroclastic material collapsed into the ocean from the eruption column. The major flood of the Congo River was also not the ultimate cause of cable damage; instead, it was subsequent turbidity currents that were triggered during spring tides that ran out along the deep-sea canyon and broke cables.

At the other end of the spectrum are much lower magnitude events, including sub-annually recurrent storms and almost continuous near-bed currents that exert recurrent or sustained, but comparatively low-level, impacts. Such low-level impacts are far more likely than extreme hazards worldwide, occurring at many locales on a (quasi) continuous basis. However, cable damage arising from low magnitude sustained impacts may not readily be attributable to a specific event, as it is due to cumulative abrasion that occurs over time. Our new analysis of exposure to metocean hazards addresses this gap by attempting to attribute more unknown faults to their (oceanographic) drivers, and mapping areas of potential hazard exposure. As a result, we suggest that a large proportion of cable faults that have not previously been attributed to a root cause (i.e. labelled as 'Unknown' in cable fault databases) likely relate to such sustained or highly repetitive low-level abrasion. Based on these case studies that span disparate scales and recurrences of events, we conclude that it is rarely the initial event that is the direct cause, and instead it is cascading hazards that ultimately explain most instances of cable damage. The hazard cascades that are set in motion may occur over relatively short time periods (e.g. minutes to hours), or over even longer time periods. For example, the sediment fluxes delivered to the Congo Canyon head by a river flood in 2019/20 are thought to explain the turbidity currents that continued to recur until 2023. This is a theme that is increasingly becoming recognised for the impacts of natural hazards on many other types of infrastructure and communities (Gill and Malamud, 2016). The results from this study will help to fill the

gap in some of the 'unknowns', and further data collection and studies such as this are valuable.

### 4.2. Network resilience and hazard mitigation measures

Considering the lengths of cable currently installed on the seafloor and how dynamic the deep ocean can be, the global subsea telecommunications network experiences remarkably few faults as a result of natural processes (1.6 million km of cable, and 1473 faults potentially attributable to natural hazards). In a large part this is because of successful application of lessons learned from past instances of damage to enhance resilience. Overall, the best practice for a resilient network is through routing to avoid high-risk areas, as well as developing redundancy through a diversity of routes (Carter, 2009). This requires detailed assessment and mapping of the potential exposure to a range of natural hazards, and designing any required maintenance schedules accordingly. The exposure to a range of natural hazards is summarised in Table 2 together with commentary on frequency and approximate proportions of cable faults related to natural causes and, where possible, recommended mitigation measures. Where extreme natural hazards are unavoidable, the access to repair vessels, cable spares and access to back-up means of communications (e.g. satellite or microwave systems) will be the most critical. On a global scale such an assessment is increasingly possible using datasets such as those outlined in this study (Fig. 7).

The enhanced risks to cables laid across submarine canyons has been known for decades, with reports of fast-moving, sediment-laden currents responsible for cable breaks observed as early as 1899 (Carter et al., 2014). While only 2.7 % of the total length of the global subsea telecommunications cables lies across submarine canyons (Fig. 7A), such locations account for a disproportionately higher number of faults due to (a) the density of cables in regions such as Taiwan and Algeria and (b) the hazards posed by turbidity currents, and so are avoided where possible. Even submarine canyons that are not directly attached to river systems or longshore sediment supplies can be extremely active sediment transport pathways, meaning they can often experience multiple density driven flows of sediment down their lengths (e.g. Heijnen et al., 2022). For example, in the Gaoping Canyon (offshore South-west Taiwan) new systems have been routed in response to the heightened threat to cables situated in canyons, following repeated instances of cable damage. This stretch has now been routed into deeper water, further from shore, where turbidity currents triggered by tropical cyclones decelerate to speeds that no longer damage cables (Carter et al., 2014). A new cable was installed in deeper water, to completely avoid the Congo Canyon and its deep-sea fan, which was the only system to survive cable damage in 2023, providing some additional capacity when the other cables were broken by turbidity currents.

Although the subsea telecommunications network is resilient on a global scale, the case studies presented here highlight how cascades of natural events can lead to widespread, and sometimes repeated, damage that can affect multiple cable systems synchronously. Telecommunications resilience is enhanced by a diversity of routes and landing stations, which reduce the likelihood that a single event will damage all connections and allowing traffic to be rerouted through undamaged cables. Such a situation may result in a reduction in bandwidth capacity regionally, but allows almost all internet services to be maintained. The diversity of routing is greater in places that have more cables, which include regions such as the North Atlantic and North-west Europe, related to their importance as centres for global finance and trade, their large populations and GDPs. However, in regions with few connections, or where cables are very closely spaced, a single natural hazard event has the potential to effectively disconnect an entire nation from the internet. Locations with the fewest connections tend also often those that are most remote, many of which are Small Island Developing States (SIDS). Many SIDS, are collocated with tectonic plate boundaries, this geological setting makes them more vulnerable to high seismicity and

**Table 2**  
Risk register of potential natural hazards to subsea cables.

Hazard	Impacts	Frequency and exposure of cable network to natural causes	Mitigation
Volcanoes	Multiple possible impacts, including: i) Hot erupted material damages cable; ii) Fast-moving density currents that enter the ocean can sever or bury cable; iii) Volcanic activity may trigger slope failure. iv) creation of rough topography v) topographic intensification of local currents	Very rare but major events located at or adjacent to submerged volcanoes.	Avoid volcanically active and passive areas where possible. Ensure diversity of cable routes and landing stations. Invest in low-level satellite communications as a back-up for remote island and coastal states in volcanically active regions.
Submarine landslides	Displacement or burial of large areas of seafloor by sometimes fast-moving slope failure and resultant sediment density flows, leading to cable damage due to drag, abrasion or excess burial.	Largest landslides (>5 km <sup>3</sup> ) tend to be rare, but smaller (<1 km <sup>3</sup> ) failures can occur more frequently.	Avoid areas that may be prone to slope failure (and downslope of those areas) where possible.
Earthquakes	Destabilisation of slopes and generation of turbidity currents that may directly impact cables.	Moderate. Focused on seismically active regions. Impacts greatest in areas that also receive high sediment supply leading to zones prone to failure.	Diversity of routes in areas affected by high seismicity. Avoid areas of high sediment accumulation and crossing of submarine canyons where possible. Otherwise accept risk.
Tsunami	Highly elevated shear stresses on continental shelf lead to abrasion and chafe or exposure of buried cables. Inundation of shore-based facilities.	Generally rare. More prone in seismically active regions (earthquake-triggered), but can also be triggered by submarine landslides and volcanic activity and travel across entire oceans.	Sufficient burial and/or physical protection of cables in areas prone to tsunami impact.  Design cable landing stations to be sufficiently elevated and able to withstand inundation. Understand compound hazards under sea-level rise
River floods	River floods discharge sediment offshore, either directly or indirectly triggering turbidity currents, leading to dragging or abrasion of cable by fast-moving flow that can travel 10s–1000s of kms that may also result in major seafloor erosion.	Common offshore from rivers (sometimes multiple flows per year), particularly those with high particulate loads and that experience heavy flooding	Avoid crossing submarine canyons and areas at the outflow of rivers. Where canyon crossing is necessary, select deeper water reaches that are broader, low relief and that avoid knickpoints (especially immediately upstream of such features).
Storms and wave action	Wave loading leading to	Multiple low-level events that	Burial of cable to a depth below seafloor

**Table 2 (continued)**

Hazard	Impacts	Frequency and exposure of cable network to natural causes	Mitigation
	liquefaction or mobilisation of seafloor sediments, abrasion and fatigue on cable. Inundation of shore-based cable facilities.	occur seasonally which can occasionally be damaging.	that cannot be mobilised by the wave base or use physical protection where cable cannot be buried.
Seafloor currents	Strumming of cable by direct interaction with current, leading to abrasion and chafe, particularly on irregular/rocky seafloor. Exposure of buried cable due to reworking of sediments by currents.	Continuous/sustained exposure to 'slow' ocean currents and fast / reversing tidal currents	Burial of cable /physical protection. Rerouting to avoid hotspots of well-mapped current action.

volcanic eruptions, while also exposed to marine and meteorological hazards. Furthermore, the low-lying topography and remote location of many such islands places them at heightened risk of the impacts of climate change, including sea-level rise, and tropical storm intensity and frequency (e.g. Meheux and Parker, 2006; Forbes et al., 2013; Nunn and Kumar, 2018; Scandurra et al., 2018). Thus, many of the world's least resilient communities are located in the regions where natural processes are most likely to damage subsea telecommunications cables. These remote communities are also often more reliant than other regions on internet connectivity because they are distant from centralised services such as education and medicine (Burnett and Carter, 2017). Thus, internet outages, particularly those that last for prolonged periods, can severely disrupt not only business and financial transactions, but almost every aspect of daily life. Oceania is particularly vulnerable (Fig. 1), with fewer connections and lower bandwidth (and some communities dependant on a single connection), yet this region is also disproportionately affected by natural hazards, with high concentrations of seismicity, volcanic activity, storms and waves (Fig. 7). Oceania is also likely to be more severely impacted by climate change, increasing the potential severity of many of these events.

In many cases, diversifying route options for SIDS is challenging because it is hard to build a business case to support multiple routes without the bandwidth demand due to low relative population densities (Kaul et al. (2024)). In designing new routes to connect previously unconnected SIDS, it may also be impossible to totally avoid marine geohazards, for example, many remote islands are themselves active volcanic centres, and therefore there is no way to avoid volcanic hazards. Therefore, in such settings better access to cable repair vessels is needed, as is holding sufficient stocks of spare cable for repairs. These contingency measures should be combined with improved low-level satellite coverage and other back-up measures, as appropriate, to increase resilience, in addition to ensuring there are geographically diverse cable routes and landing station options. Any new system should have as much onward connectivity as possible for commercial reasons, so ideally it lands close to other cables which connect to places outside the scope of the new system. This enhances overall network resilience as traffic can easily be switched, but does encourage a single point of failure for that landing/country.

There are other challenges for subsea telecommunications network resilience. It is hard to design a network resilient to previously unexperienced hazards, for example very rare but high magnitude events such as the 2022 eruption of Hunga volcano. High magnitude events



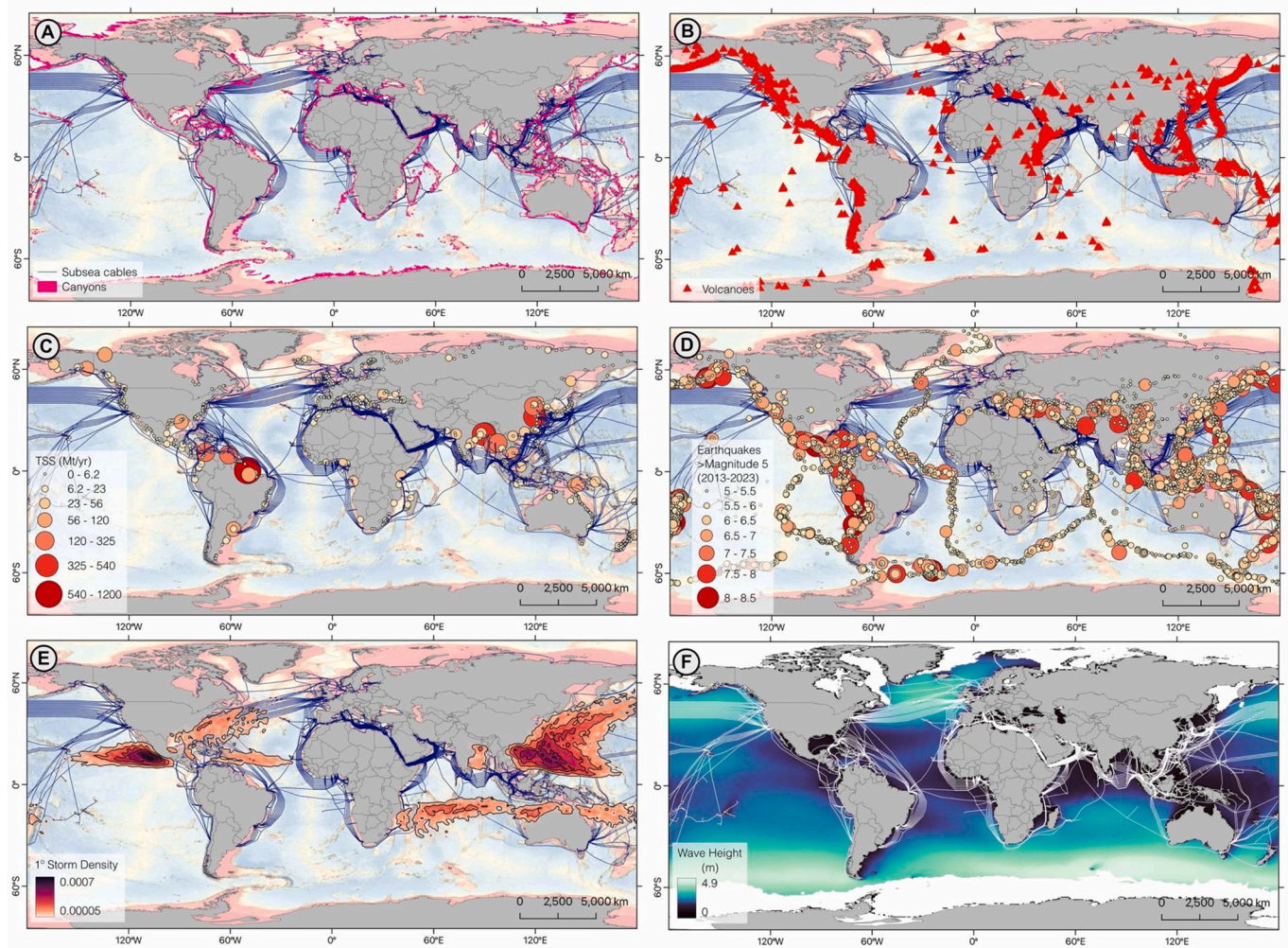


**Fig. 7.** Maps of cable locations and the distribution of natural hazards referenced in this study. [A] The locations of submarine canyons, the most hazardous seafloor locations for cable damage (Global seafloor morphology). [B] Indication of the volcanic active regions (Smithsonian database); [C] Total suspended sediment transported yearly by major rivers (Milliman Farnsworth database); [D] Significant seismicity (USGS); [E] Locations and density of tropical storms (IBTrACS); and mean significant wave height (m) over 37-year hind cast.

tend to generate extreme seafloor changes, in this case long runout, dense, high-velocity submarine flows (Clare et al., 2023; Seabrook et al., 2023). However, their scale means that to avoid such seabed flows would likely require substantial investment, whilst their frequency (e.g. ~1:100 s–1000s of years) compared to the design life of a subsea telecommunications cable (~25 years), coupled with a lack of monitoring to forecast future events, means that it is unlikely to make financial sense to attempt to route to avoid similar events. Again, contingency in the form of access to repair vessels, availability of spare cable and satellite coverage is more viable than route design or diversity, although improved seafloor monitoring and mapping could aid in identifying regions that are more likely to experience major events, and therefore where there may be a financial case for rerouting.

The development of new routes, where there is no prior cable routing experience, also presents a challenge for identifying natural hazard-related threats to subsea cables. For example, new cable routes crossing into high latitudes are being developed to meet new network requirements, and because these regions are increasingly accessible as a result of anthropogenic climate change. There is an increased risk of ice-related cable damage to such high latitude cables. These high latitude regions are often more poorly mapped than in lower latitudes, so that the distribution and frequency of hazards are less well known. Improved and repeated seafloor mapping in these regions, in particular using vessel mounted multibeam systems, would enable better cable routing

and a fuller understanding of the diversity and frequency of hazards that may occur.

#### 4.3. Addressing research gaps

Industry-based databases that record the timing and location of instances where a cable has been damaged and/or required repair are extremely valuable; however, such databases provide only binary information. Where a natural hazard event causes instantaneous damage, attribution is straightforward. But this database will miss two other more nuanced situations; where external events occurred but were not sufficient to cause a fault; and also those that do not instantaneously result in damage, but may do so cumulatively over time. There remain instances where multiple cables have experienced the same event, but some cables survived intact, whilst other cables were damaged. Examples include the 2020 Congo Canyon turbidity currents where one cable remained unaffected, while all other cable systems were broken (Talling et al., 2022a, 2022b), and following the 2006 Pingtung earthquake where several cables that crossed the Gaoping Canyon remained undamaged, while others were cut (Carter et al., 2012; Gavey et al., 2017). The reasons why some cables may survive remain unclear, largely due to a lack of sufficiently detailed contextual data: In some cases (especially historically) the database may not be complete where the cables are maintained by different companies or zone agreements. It is

hypothesised that in these cases, local topography and patchy seabed erosion by turbidity currents may provide an explanation (Pope et al., 2022; Talling et al., 2022a, 2022b). Flows may have slowed down where they were steered or protected by topography, or due to the interaction of the flow with the seabed that locally eroded deep scours downstream of steep steps in the canyon profile (called knickpoints) that migrated upstream (Heijnen et al., 2020; Pope et al., 2022), potentially leaving some cables exposed or even suspended above the canyon axis. Otherwise, the effects of burial by sediment carried by earlier non-damaging flows may have shielded cables from the subsequent more powerful flow. These are examples of cascading hazards where it is not immediately apparent why some cables survived and others broke, underlining a need for gathering and sharing of more contextual data (e.g. Carter et al., 2014; Gavey et al., 2017).

4.3.1. Gaps in our understanding of hazard predictability and forecasting

There are limits on the predictability and forecasting of different categories of natural hazards, which inform the research gaps. Fig. 8 presents a schematic illustration of the spectrum of cascading hazards scenarios that create cable damage, and a summary risk register of the consequences and likelihood of each natural hazard. We now discuss these different hazards, that include geological, hydrological, meteorological, and oceanographic aspects.

Geological hazards originate from events such as earthquakes,

volcanic eruptions, submarine landslides, and tsunamis, which may be independent or dependent on each other. Such events are currently largely unpredictable and in many cases are unavoidable. In such cases, the most appropriate mitigation methods may be detailed seafloor mapping and route characterisation to identify optimal routes, and monitoring of hazards, or the drivers of those hazards, that may enable early warning. The frequency of earthquakes, tsunamis, and volcanic eruptions is unlikely to change rapidly in the near-future as they occur independently of climate change; however, submarine landslides and associated turbidity currents may be affected by changes in sea level, temperature and sediment fluxes that are modulated and may lag behind climate change.

Hydrological hazards include events such as river floods and the subsequent turbidity currents that they can generate, but may also include delivery of sediment offshore to trigger landslides (Pope et al., 2017b). Inland monitoring of river discharge, and observations of seabed change can improve mapping of risk and may permit offshore predictions in some specific settings (e.g. Bailey et al., 2023). Such events may increase in frequency in the future, due to more intense rainfall events driven by climate change in addition to the implications of human changes to river catchments that can exacerbate flooding and sediment runoff events (Frich et al., 2002; Trenberth, 2011; Nienhuis et al., 2020; Talling et al., 2022a, 2022b). Higher resolution meteorological models, and climate downscaling can also improve predictability

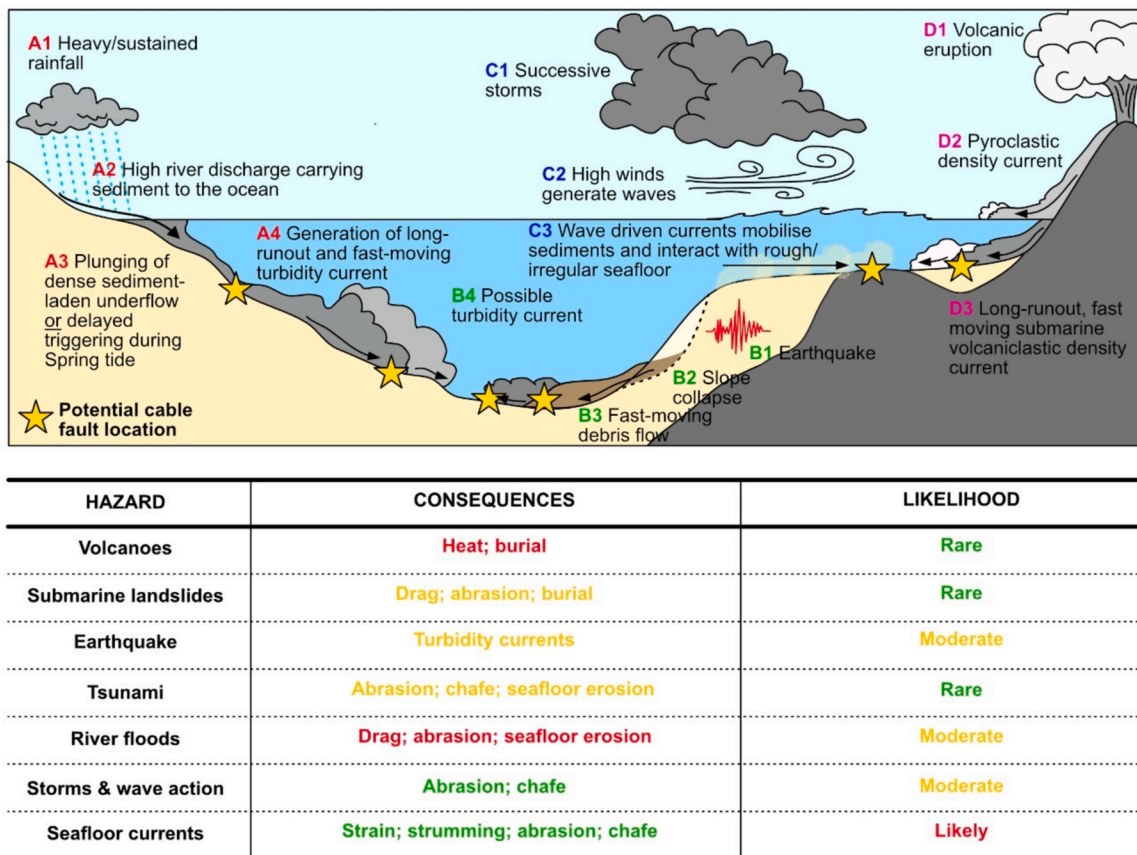


Fig. 8. [upper panel] Schematic illustration of different cascading hazards scenarios that create cable damage (shown as yellow stars) can arise in different settings, including: A) sequences of events resulting from tropical cyclones such as seen offshore south-west Taiwan, where cable damage can be delayed by days to weeks after the passage of a storm (Carter et al., 2014); B) earthquake-related damage that results from cascades of mass movements that are triggered by the ground shaking, which can occur hundreds of kilometres away from the earthquake epicentre (e.g. Boxing Day 2004 earthquake in the Andaman Sea and 2011 Tohoku-Oki quake in Japan (Pope et al., 2017a, 2017b); C) Progressive exposure and abrasion of previously-buried cable by sustained near bed currents or (as shown) sequential elevations in near-bed shear stresses resulting from repeated storms); D) Volcanic eruptions may damage cables directly by the eruption, by pyroclastic density currents which may damage landing stations and shallow infrastructure, or by the entry of volcanic material into the marine environment as submarine density flows. This is not intended as a comprehensive overview; simply to highlight some of the complex hazards cascades that can exist in different settings. [lower panel] Risk register coloured by the severity of the consequence; minor (green), major (amber), or extreme (red) and likelihood; rare (green), moderate (amber), and common (red).



of high intensity rainfall events (e.g. Schmidli et al., 2006).

Meteorological hazards driven directly by atmospheric processes and weather phenomena (hurricanes, tornadoes, mid-latitude cyclones and typhoons) can generate large sea-waves. These storms are sporadic, but predictable in both timing, track, and intensity (e.g. Roy and Kovordányi, 2012). The latest generation of climate models has improved representation of storms, and downscaling with parametric models can also improve the predictability of hurricane impacts. Tools are available to translate surface wave energy to a physical seabed stress (e.g. Aldridge et al., 2015), and we can map the exposure of seabed to wave energy. Better climate prediction can also quantify the changing storm tracks, and strength and frequency of extreme events in the context of the climate crisis.

With regards to oceanographic hazards, exposure to seafloor stress from the majority of seafloor currents is regular and highly predictable, be it via slow deep ocean currents, or fast reversing shelf-sea tides. However periodic benthic storms may generate fast (>0.2 m/s) currents for a few days causing erosion and potential cable movement followed by a return to the prevailing slow deep ocean current. In-situ monitoring is available at some locations, but numerical models may be the only available data source across much of the (deep) ocean. High-resolution modelling data can be of great value in robustly guiding future route assessments. With accurate seabed maps, the simulated currents are only as good as permitted by numerical model resolution (Mayer et al., 2018). Canyon features will not be resolved at a spatial scale of global hydrodynamic model resolution (the order 10 km). Regional models with resolution of the order 10s–100s m are required to accurately capture the complex and sharp seabed shape and associated currents. Numerical models can also have poor-performance around steep topography due to insufficient vertical resolution. This is a clear area for future work, with increased model capability we will be better able to deliver higher-resolution maps, to calculate (and mitigate against) the risk to cables from fast seabed current and interactions with bottom topography.

It is important to recognise that this mapping of exposure to seabed currents and waves is a relative, rather than absolute, assessment on a global scale. An absolute measure of seabed stress is not meaningful to calculate globally, as this depends on the sediment type, or object that is experiencing the force. As well as the deep ocean currents, large tidal currents dominate some shelf seas, and in shallow water. Fast, oscillating tidal flow can cause large stresses at the seabed (e.g. Aldridge et al., 2015). Both the current speed and angle of incidence are important, as currents acting across currents will exert more force. A typical double armoured cable will be moved by a current velocity in excess of 0.5 m/s when acting at 90 degrees to the axis of the cable (Griffiths and Lucas, 2021). Regular tidal currents experienced in shelf seas (e.g. around North-west Europe) can regularly exceed this value, reaching speeds of over 1.5 m/s during a typical month (Byrne et al., 2023) in areas of shallow water. There is also a risk from strong tidal currents moving around headlands and through straits. Cables are often laid across these straits, as these narrow areas represent the shortest route and thus are the most exposed.

As a result of ongoing human-driven climate change, there is an increase in frequency and severity of intense tropical cyclones on a global basis (Emanuel, 2021). Furthermore, the shifting positions of future storm tracks will also alter the locations at risk from seabed disturbance by storm waves. Changing wave climate will also combine with sea-level rise (which increases water depth in an uneven way across the globe). At first order, deeper water will uncouple the energetic surface waves from the seabed, reducing the risk. However, deeper water also allows long waves to travel further unchecked, which will alter the geographic areas at risk from these waves. Rising sea-levels may also inundate parts of the coast, and alter the water depths in which the cables are laid. In addition, sea-level rise can also alter the movement of the tides (e.g. Pickering et al. (2012), thereby changing the position and strength of seabed currents. For more on how climate change may potentially affect seabed

cables in the future see Clare et al. (2023).

#### 4.3.2. Gaps in our understanding of seafloor variability in time and space

Detailed multibeam bathymetric surveys provide enhanced understanding of local-scale seafloor relief, which can identify previously uncharacterised hazardous terrain. For example, outcropping bedrock or corals that may enhance the potential for abrasion, and bedforms that provide an indication of past (and potentially ongoing) flow behaviour and pathways, which may be indicative of seafloor hazards. Repeat seafloor surveys, coupled with direct monitoring, can provide further insights into the nature of seafloor processes as has been clearly demonstrated offshore Tonga and in the Congo Canyon (Seabrook et al., 2023; Pope et al., 2022). The availability of sufficiently high-resolution bathymetric data is a key ingredient in more robustly diagnosing cable faults and in informing future route assessments. There is a compelling need to gather higher resolution bathymetry data, as well as fundamentally filling in gaps where no detailed data exist at all. Only one quarter of the seabed has been mapped globally to date (gebco.net), with global data compiled in the General Bathymetric Chart of the Oceans (GEBCO; Weatherall et al., 2015). There is ongoing effort to meet this need through projects such as Seabed 2030 (Mayer et al., 2018).

## 5. Conclusions

The subsea cable industry goes to great lengths to ensure the resilience of the network and reduce the occurrence of faults. Aside from human activities (especially fishing and shipping), the remaining threat to network resilience primarily comes from natural hazards. Across the global ocean, subsea cables are exposed to every category of natural hazard. While extreme geological events are rare, they can cause catastrophic, and widespread damage to cables. More (apparently benign) hydrological and oceanographic processes, can still threaten the network, but crucially are more predictable and better understood. Through attribution of historical cable faults to environmental processes, we can present a more complete picture of the risk posed by natural hazards. Our understanding of these oceanographic risk factors can help identify highly exposed and vulnerable areas in order to continue future-proofing the globally-critical telecommunications infrastructure against the impacts of natural hazards and the creeping effects of ongoing climate change.

## Declaration of competing interest

The authors declare that they have no known competing financial interests or personal relationships that could have appeared to influence the work reported in this paper.

## Acknowledgements

This work was supported by Natural Environment Research Council grant NE/X00239X/1 (M.A.C. and I.A.Y.); Natural Environment Research Council grant NE/X003272/1 (J.E.H., M.A.C., and I.A.Y.); International Cable Protection Committee (M.A.C. and I.A.Y.). L.B. and M.A.C. acknowledge funding from NERC National Capability Programme (NE/R015953/1) “Climate Linked Atlantic Sector Science”. L. B., M.A.C, J.H., and I.A.Y acknowledge funding from UK Research and Innovation (UKRI) COP26 research grant 2021COPA&R22Clare and support from Victoria University of Wellington (to L.C). Map data for cable network and landing sites were provided by TeleGeography. Thanks also go to Brian Perratt (OceanIQ) for providing information on past cable faults caused by natural hazards.

## Data availability

Data will be made available on request.

## References

- Aldridge, J.N., Parker, E.R., Bricheno, L.M., Green, S.L., Van Der Molen, J., 2015. Assessment of the physical disturbance of the northern European Continental shelf seabed by waves and currents. *Cont. Shelf Res.* 108, 121–140.
- Allan, P.G., 2000. Cable security in sandwaves. In: *Proceedings of the International Cable Protection Committee Plenary Meeting, Copenhagen*.
- Aller, J.Y., 1989. Quantifying sediment disturbance by bottom currents and its effect on benthic communities in a deep-sea western boundary zone. *Deep Sea Res. A* 36 (6), 901–934.
- Bailey, L.P., Clare, M.A., Rosenberger, K.J., Cartigny, M.J.B., Talling, P.J., Paull, C.K., Gwiazda, R., Parsons, D.R., Simmons, S.M., Xu, J., Haigh, I.D., Maier, K.L., McGann, M., Lundsten, E., 2021. Preconditioning by sediment accumulation can produce powerful turbidity currents without major external triggers. *Earth Planet. Sci. Lett.* 562, 116845. <https://doi.org/10.1016/j.epsl.2021.116845>.
- Bailey, L.P., Clare, M.A., Pope, E.L., Haigh, I.D., Cartigny, M.J.B., Talling, P.J., Lintern, D. G., Hage, S., Heijnen, M., 2023. Predicting turbidity current activity offshore from meltwater-fed river deltas. *Earth Planet. Sci. Lett.* 604, 117977.
- Bricheno, L.M., Wolf, J., 2018. Future wave conditions of Europe, in response to high-end climate change scenarios. *J. Geophys. Res. Oceans* 123, 8762–8791.
- Burnett, D.R., Carter, L., 2017. *International Submarine Cables and Biodiversity of Areas beyond National Jurisdiction: The Cloud beneath the Sea*. Brill.
- Byrne, D., Polton, J., Bell, C., 2023. Creation of a global tide analysis dataset: application of NEMO and an offline objective analysis scheme. *J. Oper. Oceanogr.* 16, 175–188. <https://doi.org/10.1080/1755876X.2021.2000249>.
- Carr III, L.E., Elsberry, R.L., 1995. Monsoonal interactions leading to sudden tropical cyclone track changes. *Mon. Weather Rev.* 123, 265–290.
- Carter, L., 2009. *Submarine Cables and the Oceans: Connecting the World*. UNEP/Earthprint.
- Carter, L., Wright, R.C., Collins, N., Mitchell, J.S., Win, G., 1991. Seafloor stability along the Cook Strait power cable corridor. In: *Australasian Conference on Coastal and Ocean Engineering*. Water Quality Centre, DSIR Marine and Freshwater, Hamilton, New Zealand, pp. 535–540.
- Carter, L., Milliman, J.D., Talling, P.J., Gavey, R., Wynn, R.B., 2012. Near-synchronous and delayed initiation of long run-out submarine sediment flows from a record-breaking river flood, offshore Taiwan. *Geophys. Res. Lett.* 39.
- Carter, L., Gavey, R., Talling, P.J., Liu, J.T., 2014. Insights into submarine geohazards from breaks in subsea telecommunication cables. *Oceanography* 27, 58–67.
- Cattaneo, A., Babonneau, N., Ratzov, G., Dan-Unterseh, G., Yelles, K., Bracene, R., Mercier De Lepinay, B., Boudiaf, A., Déverche, J., 2012. Searching for the seafloor signature of the 21 May 2003 Boumerdes earthquake offshore Central Algeria. *Nat. Hazards Earth Syst. Sci.* 12, 2159–2172.
- Clare, M.A., Clarke, J.E.H., Talling, P.J., Cartigny, M.J.B., Pratomo, D.G., 2016. Preconditioning and triggering of offshore slope failures and turbidity currents revealed by most detailed monitoring yet at a fjord-head delta. *Earth Planet. Sci. Lett.* 450, 208–220.
- Clare, M.A., Yeo, I.A., Bricheno, L., Aksenov, Y., Brown, J., Haigh, I.D., Wahl, T., Hunt, J., Sams, C., Chaytor, J., 2022. Climate change hotspots and implications for the global subsea telecommunications network. *Earth Sci* 237, 104296.
- Clare, M.A., Yeo, I.A., Watson, S., Wysoczanski, R., Seabrook, S., Mackay, K., Hunt, J.E., Lane, E., Talling, P.J., Pope, E., Cronin, S., Ribó, M., Kula, T., Tappin, D., et al., 2023. Fast and destructive density currents created by ocean-entering volcanic eruptions. *Science* 381, 1085–1092. <https://doi.org/10.1126/science.adi3038>.
- Dinmohammadi, F., Flynn, D., Bailey, C., Pecht, M., Yin, C., Rajaguru, P., Robu, V., 2019. Predicting damage and life expectancy of subsea power cables in offshore renewable energy applications. *IEEE Access* 7, 54658–54669.
- Emanuel, K., 2021. Response of global tropical cyclone activity to increasing CO<sub>2</sub>: results from downscaling CMIP6 models. *J. Clim.* 34, 57–70.
- Ericson, D.B., Ewing, M., Heezen, B.C., 1952. Turbidity currents and sediments in North Atlantic. *AAPG Bulletin* 36 (3), 489–511.
- Forbes, D.L., James, T.S., Sutherland, M., Nichols, S.E., 2013. Physical basis of coastal adaptation on tropical small islands. *Sustain. Sci.* 8, 327–344.
- Frich, P., Alexander, L.V., Della-Marta, P., Gleason, B., Haylock, M., Tank, A.M.G.K., Peterson, T., 2002. Observed coherent changes in climatic extremes during the second half of the twentieth century. *Clim. Res.* 19, 193–212.
- Gallina, V., Torresan, S., Critto, A., Sperotto, A., Glade, T., Marcomini, A., 2016. A review of multi-risk methodologies for natural hazards: Consequences and challenges for a climate change impact assessment. *J. Environ. Manag.* 168, 123–132.
- Gardner, W.D., Tucholke, B.E., Richardson, M.J., Biscaye, P.E., 2017. Benthic storms, nepheloid layers, and linkage with upper ocean dynamics in the western North Atlantic. *Mar. Geol.* 385, 304–327.
- Gavey, R., Carter, L., Liu, J.T., Talling, P.J., Hsu, R., Pope, E., Evans, G., 2017. Frequent sediment density flows during 2006 to 2015, triggered by competing seismic and weather events: Observations from subsea cable breaks off southern Taiwan. *Mar. Geol.* 384, 147–158.
- GDIP, 2024. *Good Practices for Subsea Cables Policy: Investing in Digital Inclusion*. Global Digital Inclusion Partnership.
- Gigacom, 2012. *Superstorm Sandy wreaks havoc on internet infrastructure*. <https://gigaom.com/2012/10/30/superstorm-sandy-wreaks-havoc-on-internet-infrastructure/>.
- Gill, J.C., Malamud, B.D., 2016. Hazard interactions and interaction networks (cascades) within multi-hazard methodologies. *Earth Syst. Dynamics* 7 (3), 659–679.
- Griffiths, A., Lucas, G., 2021. Improving Cable Landfall Resiliency through Abrasion Risk Analysis. *International Cable Protection Committee Plenary*.
- Hampton, M.A., Lee, H.J., Locat, J., 1996. Submarine landslides. *Rev. Geophys.* 34, 33–59.
- Harris, P.T., Whiteway, T., 2011. Global distribution of large submarine canyons: Geomorphic differences between active and passive continental margins. *Mar. Geol.* 285 (1–4), 69–86.
- Heezen, B.C., Johnson, G.L., 1969. Alaskan submarine cables: a struggle with a harsh environment. *Arctic* 413–424.
- Heezen, B.C., Menzies, R.J., Schneider, R.J., Ewing, W.M., Graneli, N.C.L., 1964. Congo submarine canyon. *AAPG Bull.* 48, 1126–1149.
- Heijnen, M.S., Clare, M.A., Cartigny, M.J.B., Talling, P.J., Hage, S., Lintern, D.G., Stacey, C., Parsons, D.R., Simmons, S.M., Chen, Y., 2020. Rapidly-migrating and internally-generated knickpoints can control submarine channel evolution. *Nat. Commun.* 11, 3129.
- Heijnen, M.S., Mienis, F., Gates, A.R., Bett, B.J., Hall, R.A., Hunt, J., Kane, I.A., Pebody, C., Huvenne, V.A.I., Soutter, E.L., 2022. Challenging the highstand-dormant paradigm for land-detached submarine canyons. *Nat. Commun.* 13, 3448.
- Hollister, C.D., McCave, I.N., 1984. Sedimentation under deep-sea storms. *Nature* 309 (5965), 220–225.
- Howe, B.M., Angove, M., Aucan, J., Barnes, C.R., Barros, J.S., Bayliff, N., Becker, N.C., Carrilho, F., Fouch, M.J., Fry, B., 2022. SMART subsea cables for observing the earth and ocean, mitigating environmental hazards, and supporting the blue economy. *Front. Earth Sci.* 9, 775544.
- Hsu, S.-K., Kuo, J., Chung-Liang, L., Ching-Hui, T., Doo, W.-B., Ku, C.-Y., Sibuet, J.-C., 2008. Turbidity currents, submarine landslides and the 2006 Pingtung earthquake off SW Taiwan. *TAO: Terr. Atmos. Ocean. Sci.* 19, 7.
- Huthnance, J.M., Humphery, J.D., Knight, P.J., Chatwin, P.G., Thomsen, L., White, M., 2002. Near-bed turbulence measurements, stress estimates and sediment mobility at the continental shelf edge. *Prog. Oceanogr.* 52, 171–194. [https://doi.org/10.1016/S0079-6611\(02\)00005-8](https://doi.org/10.1016/S0079-6611(02)00005-8).
- Kaul, A., Ng, M., Ting Toh, J., Goh, L., 2024. *Connecting Fiji: The opportunity for growth and prosperity from subsea internet investment*. <https://accesspartnership.com/connecting-fiji-the-opportunity-for-growth-and-prosperity-from-subsea-internet-investment/>.
- Knapp, K.R., Kruk, M.C., Levinson, D.H., Diamond, H.J., Neumann, C.J., 2010. The international best track archive for climate stewardship (IBTrACS) unifying tropical cyclone data. *Bull. Am. Meteorol. Soc.* 91, 363–376.
- Kordahi, M., Shapiro, S., 2004. *Worldwide Trends in Submarine Cable System Faults*, SubOptic, May 2004, Monte Carlo, Monaco. <http://suboptic.org/resources/>.
- Kordahi, M.E., Shapiro, S., Lucas, G., 2007. *Trends in Submarine Cable System Faults*, SubOptic, 2007, Baltimore, MD. <http://suboptic.org/resources/>.
- Kordahi, M.E., Stix, R.K., Rapp, R.J., Sheridan, S., Lucas, G., Wilson, S., Perratt, B., 2016. Global trends in submarine cable system faults, SubOptic, 2016, Dubai. <https://suboptic.org/wp-content/uploads/fromkevin/program/TU3B.4%20Global%20Trends%20in%20Submarine%20Cable%20System%20Faults.pdf>.
- Kordahi, M.E., Rapp, R.J., Stix, R.K., Sheridan, S., Irish, O.B., Wall, D., Waterworth, G., Perratt, B., Wilson, S., Holden, S., 2019. Global trends in submarine cable system faults, 2019 Update. *SubOptic, 2019*, New Orleans. [https://suboptic2019.com/suboptic-2019-papers-archive/Session OP8-1](https://suboptic2019.com/suboptic-2019-papers-archive/Session%20OP8-1).
- Lasley, C.B., Simpson, D.M., Rockaway, T.D., Weigel, T., 2007. Understanding critical infrastructure failure: examining the experience of Biloxi and Gulfport Mississippi after Hurricane Katrina. *Int. J. Crit. Infrastruct.* <https://doi.org/10.1504/IJCIS.2010.033339>.
- Lynett, P., McCann, M., Zhou, Z., Renteria, W., Borrero, J., Greer, D., Fa'anunu, O., Bosserele, C., Jaffe, B., La Selle, S., Ritchie, A., 2022. Diverse tsunamigenesis triggered by the Hunga Tonga-Hunga Ha'apai eruption. *Nature* 609 (7928), 728–733.
- Madsen, O.S., Wright, L.D., Boon, J.D., Chisholm, T.A., 1993. Wind stress, bed roughness and sediment suspension on the inner shelf during an extreme storm event. *Cont. Shelf Res.* 13, 1303–1324.
- Mayer, L., Jakobsson, M., Allen, G., Dorschel, B., Falconer, R., Ferrini, V., Lamarche, G., Snaith, H., Weatherall, P., 2018. The Nippon Foundation—GEBCO seabed 2030 project: the quest to see the world's oceans completely mapped by 2030. *Geosciences* 8, 63.
- Meheux, K., Parker, E., 2006. Tourist sector perceptions of natural hazards in Vanuatu and the implications for a small island developing state. *Tour. Manag.* 27, 69–85.
- Milliman, J.D., Farnsworth, K.L., 2013. *River Discharge to the Coastal Ocean: A Global Synthesis*. Cambridge University Press.
- Morton, S., Pencheon, D., Squires, N., 2017. Sustainable Development Goals (SDGs), and their implementation: a national global framework for health, development and equity needs a systems approach at every level. *Br. Med. Bull.* 124 (1), 81–90.
- Nienhuis, J.H., Ashton, A.D., Edmonds, D.A., Hoitink, A.J.F., Kettner, A.J., Rowland, J. C., Törnqvist, T.E., 2020. Global-scale human impact on delta morphology has led to net land area gain. *Nature* 577, 514–518.
- Normandeau, A., MacKillop, K., Macquarrie, M., Richards, C., Bourgault, D., Campbell, D.C., Maselli, V., Philibert, G., Clarke, J.H., 2021. Submarine landslides triggered by iceberg collision with the seafloor. *Nat. Geosci.* 14, 599–605.
- Nunn, P., Kumar, R., 2018. Understanding climate-human interactions in Small Island developing States (SIDS) implications for future livelihood sustainability. *Int. J. Clim. Chang. Strateg. Manag.* 10, 245–271.
- Pakokung, K., Suppasri, A., Imamura, F., 2022. The near-field tsunami generated by the 15 January 2022 eruption of the Hunga Tonga-Hunga Ha'apai volcano and its impact on Tongatapu, Tonga. *Sci. Rep.* 12 (1), 15187.
- Pickering, M.D., Wells, N.C., Horsburgh, K.J., Green, J.A.M., 2012. The impact of future sea-level rise on the European Shelf tides. *Cont. Shelf Res.* 35, 1–15.
- Piper, D.J.W., Cochonat, P., Morrison, M.L., 1999. The sequence of events around the epicentre of the 1929 Grand Banks earthquake: initiation of debris flows and turbidity current inferred from sidescan sonar. *Sedimentology* 46, 79–97.

- Pope, E.L., Talling, P.J., Carter, L., 2017a. Which earthquakes trigger damaging submarine mass movements: insights from a global record of submarine cable breaks? *Mar. Geol.* 384, 131–146. <https://doi.org/10.1016/j.margeo.2016.01.009>.
- Pope, E.L., Talling, P.J., Carter, L., Clare, M.A., Hunt, J.E., 2017b. Damaging sediment density flows triggered by tropical cyclones. *Earth Planet. Sci. Lett.* 458, 161–169. <https://doi.org/10.1016/j.epsl.2016.10.046>.
- Pope, E.L., Heijnen, M.S., Talling, P.J., Jacinto, R.S., Gaillot, A., Baker, M.L., Hage, S., Hasenhüdl, M., Heerema, C.J., McGhee, C., 2022. Carbon and sediment fluxes inhibited in the submarine Congo Canyon by landslide-damming. *Nat. Geosci.* 15, 845–853.
- Pope, E.L., Talling, P.J., Carter, L., Clare, M.A., Hunt, J.E., 2017. Damaging sediment density flows triggered by tropical cyclones. *Earth Planet. Sci. Lett.* 458, 161–169.
- Proud, S.R., Prata, A.T., Schmauß, S., 2022. The January 2022 eruption of Hunga Tonga-Hunga Ha'apai volcano reached the mesosphere. *Science* 378 (6619), 554–557.
- QGIS Development Team, 2020. QGIS Geographic Information System. Open Source Geospatial Foundation Project.: v. <http://qgi>.
- Rayleigh, L., 1880. On the stability, or instability, of certain fluid motions. *Proc. Lond. Math. Soc.* 9, 57–70.
- Riley, S.J., DeGloria, S.D., Elliot, R., 1999. Index that quantifies topographic heterogeneity. *Intermountain J. Sci.* 5, 23–27.
- Roy, C., Kovordányi, R., 2012. Tropical cyclone track forecasting techniques—A review. *Atmos. Res.* 104, 40–69.
- Scandurra, G., Romano, A.A., Ronghi, M., Carfora, A., 2018. On the vulnerability of Small Island Developing States: a dynamic analysis. *Ecol. Indic.* 84, 382–392.
- Schmidli, J., Frei, C., Vidale, P.L., 2006. Downscaling from GCM precipitation: a benchmark for dynamical and statistical downscaling methods. *Int. J. Climatol.* 26, 679–689.
- Seabrook, S., Mackay, K., Watson, S., Clare, M., Hunt, J., Yeo, I., Lane, E., Clark, M., Wysoczanski, R., Rowden, A., 2023. Pyroclastic Density Currents Explain Far-Reaching and Diverse Seafloor Impacts of the 2022 Hunga Tonga Hunga Ha'apai Eruption.
- Smith, W.H., Sandwell, D.T., 1997. Global sea floor topography from satellite altimetry and ship depth soundings. *Science* 277 (5334), 1956–1962.
- Snodgrass, F.E., Hasselmann, K.F., Miller, G.R., Munk, W.H., Powers, W.H., 1966. Propagation of ocean swell across the Pacific. *Philos. Trans. Royal Soc. Lond. Ser. A Math. Phys. Sci.* 259 (1103), 431–497.
- Talling, P., Baker, M., Pope, E., Jacinto, R.S., Heijnen, M., Hage, S., Simmons, S., Hasenhüdl, M., Heerema, C., Ruffell, S., 2022a. Flood and Tides Trigger Longest Measured Sediment Flow that Accelerates for Thousand Kilometers into Deep-Sea.
- Talling, P.J., Baker, M.L., Pope, E.L., Ruffell, S.C., Jacinto, R.S., Heijnen, M.S., Hage, S., Simmons, S.M., Hasenhüdl, M., Heerema, C.J., 2022b. Longest sediment flows yet measured show how major rivers connect efficiently to deep sea. *Nat. Commun.* 13, 4193.
- Tanguy, J.-C., 1994. The 1902–1905 eruptions of Montagne Pelée, Martinique: anatomy and retrospection. *J. Volcanol. Geotherm. Res.* 60, 87–107.
- Tolman, H.L., 2009. User manual and system documentation of WAVEWATCH III TM version 3.14: Technical note, MMAB Contribution, 276.
- Trenberth, K.E., 2011. Changes in precipitation with climate change. *Clim. Res.* 47, 123–138.
- Venzke, E., 2013. Global Volcanism Program. Volcanoes of the World. <https://doi.org/10.5479/si.GVP.VOTW4-2013>.
- Weatherall, P., Marks, K.M., Jakobsson, M., Schmitt, T., Tani, S., Arndt, J.E., Rovere, M., Chayes, D., Ferrini, V., Wigley, R., 2015. A new digital bathymetric model of the world's oceans. *Earth Space Sci.* 2, 331–345.
- Wilson, S., 2013. Risk to Subsea cables in the Arctic. SubOptic 2013, Paris. <https://suboptic.org/resources/suboptic-2013/>.
- WIOCC, 2023. WIOCC restores major ISPs and IP Transit providers on Equiano cable. <https://wiocc.net/blog/wiocc-restores-major-isps-and-ip-transit-providers-on-equiano-cable/>.
- Woodgate, R.A., Fahrback, E., 1999. Benthic storms in the Greenland Sea. *Deep-Sea Res. I Oceanogr. Res. Pap.* 46 (12), 2109–2127.
- Ye, L., Kanamori, H., Rivera, L., Lay, T., Zhou, Y., Sianipar, D., Satake, K., 2020. The 22 December 2018 tsunami from flank collapse of Anak Krakatau volcano during eruption. *Sci. Adv.* 6 (3) p.eaaz1377.
- Zenk, W., 2008. Abyssal and contour currents. *Dev. Sedimentol.* 60, 35–57.